Numerical Analysis and Simulation of Stochastic Partial Differential Equations with White Noise Dispersion

André Berg

UMEÅ UNIVERSITY

Department of Mathematics and Mathematical statistics
Umeå University
SE-901 87 Umeå
Sweden

Doctoral Thesis No. 75/23

ISBN Printed version: 978-91-8070-140-2
ISBN Digital version: 978-91-8070-141-9
ISSN: 1653-0810

Electronic version available at `https://umu.diva-portal.org`
Printed by CityPrint i Norr AB
Umeå, Sweden, 2023

Abstract

This doctoral thesis provides a comprehensive numerical analysis and exploration of several stochastic partial differential equations (SPDEs). More specifically, this thesis investigates time integrators for SPDEs with white noise dispersion.

The thesis begins by examining the stochastic nonlinear Schrödinger equation with white noise dispersion (SNLSE), see Paper 1. The investigation probes the performance of different numerical integrators for this equation, focusing on their convergences, L^2-norm preservation, and computational efficiency. Further, this thesis thoroughly investigates a conjecture on the critical exponent of the SNLSE, related to a phenomenon known as blowup, through numerical means.

The thesis then introduces and studies exponential integrators for the stochastic Manakov equation (SME) by presenting two new time integrators - the explicit and symmetric exponential integrators - and analyzing their convergence properties, see Paper 2. Notably, this study highlights the flexibility and efficiency of these integrators compared to traditional schemes. The narrative then turns to the Lie–Trotter splitting integrator for the SME, see Paper 3, comparing its performance to existing time integrators. Theoretical proofs for convergence in various senses, alongside extensive numerical experiments, shed light on the efficacy of the proposed numerical scheme. The thesis also deep dives into the critical exponents of the SME, proposing a conjecture regarding blowup conditions for this SPDE.

Lastly, the focus shifts to the stochastic generalized Benjamin–Bona–Mahony equation, see Paper 4. The study introduces and numerically assesses four novel exponential integrators for this equation. A primary finding here is the superior performance of the symmetric exponential integrator. This thesis also offers a succinct and novel method to depict the order of convergence in probability.

List of appended papers

Paper 1: A. Berg, D. Cohen, and G. Dujardin. "Numerical study of nonlinear Schrödinger equations with white noise dispersion". In: *N/A* (2023)

Paper 2: A. Berg, D. Cohen, and G. Dujardin. "Approximated exponential integrators for the stochastic Manakov equation". In: *Journal of Computational Dynamics* (2023). ISSN: 2158-2491. DOI: 10.3934/jcd.2023002

Paper 3: A. Berg, D. Cohen, and G. Dujardin. "Lie–Trotter splitting for the nonlinear stochastic Manakov system". In: *Journal of Scientific Computing* 88.1 (2021), pp. 1–31. DOI: 10.1007/s10915-021-01514-y

Paper 4: A. Berg. "Numerical simulations of stochastic generalized Benjamin–Bona–Mahony equations". In: *N/A* (2023)

Acknowledgments

First, I would like to thank my principal supervisor, David Cohen. His patience and efforts have, without a doubt, made me a better researcher and writer. His willingness to step up his support, sometimes to his detriment, has not been taken for granted. I also want to thank him for leading me to taste the best pizza, by far, I've ever eaten.

I want to thank my assistant supervisor, Guillaume Dujardin. He provided many vital comments that cut to the core of several issues. I've enjoyed the challenges posed and the avenues I was not previously aware of.

I wish to thank my assistant supervisor, Per Åhag. Without his welcoming office, tasty licorice, and cheerful gossip, I would have had a much rougher time. If I were to include every aspect of how he helped, I would need an itemized list to keep track of it.

I also want to thank Annika Lang, who assisted in proofreading during the thesis drafting. Despite the short time window, her comments made a significant difference.

Thanks to Klara Leffler and Niklas Fries for our entertaining and exciting discussions. Visiting Klara's office has always made me smile, and sharing the office with Niklas has both widened my horizons and deepened my existing interests.

I want to thank my wife Veronica and son Alfred. Veronica makes every day better, and every evening I spend reading with Alfred reminds me of my happiness. I hope to repay their patience during these years.

I also don't want to forget my good friends, Linnéa Gräns Samuelsson and Henrik Vestin. While geographical distance means we rarely meet, simply chatting gives me a new perspective and renewed vigor.

Lastly, I thank my remaining family, colleagues, and friends. While not mentioned by name, for brevity's sake, know that many of you deserve thanks.

List of abbreviations

	Equations
PDE	Partial differential equation
SPDE	Stochastic partial differential equation
NLSE	Nonlinear Schrödinger equation
SNLSE	Stochastic nonlinear Schrödinger equation with white noise dispersion
PMD	Polarization mode dispersion
MPMDE	Manakov PMD equation
SME	Stochastic Manakov equation
BBM	Benjamin–Bona–Mahony equation
SBBM	Stochastic generalized Benjamin–Bona–Mahony equation
KdV	Korteweg–de Vries equation
RLW	Regularized long wave equation
	Spatial discretizations
FD	Finite difference
PS	Pseudospectral
	Time integrators
MP	Midpoint Euler integrator
CN	Crank–Nicolson integrator
EE	Explicit exponential integrator
BE	Backward exponential integrator
ME	Midpoint exponential integrator
SE	Symmetric exponential integrator
LT	Lie–Trotter splitting integrator
ST	Strang splitting integrator
	Probability theory
CDF	Cumulative distribution function

Contents

1 Introduction

The advancement of mathematical modeling stands as a crucial catalyst for humanity's progress, enabling the description, comprehension, and utilization of a wide range of phenomena. Population dynamics, investment finance, satellite orbital stability, and structural mechanics are examples of the many domains that benefit from mathematical modeling [60]. Recent advancements in many fields, including modeling weather, pollution, or turbulence [53], have been significantly enhanced by using stochastic partial differential equations (SPDEs) and their numerical studies, bringing together three distinct and essential areas of inquiry.

The first of these three areas is differential equations. Since the late 17th century, differential equations have been used to describe quantities in terms of their rates of change [59]. This framework has continually generated new research and applications, including springs, string vibrations, and even the shape of suspended ropes. As the area matured, it naturally extended into partial differential equations (PDEs) and stochastic (partial) differential equations.

The second area of inquiry is stochastic analysis, which studies random processes as they evolve. This approach has proven particularly effective in addressing the challenges posed by fluctuations in observation, such as oscillations, vibrations, environmental factors, or measurement errors. In this thesis, we mainly consider white noise perturbation. It is a random property intimately tied to the Brownian motion, an idea first introduced by Louis Bachelier in the early 20th century and later utilized by Einstein [6].

The third area of inquiry, computational mathematics, is equally critical

to the success of mathematical modeling of complex problems. Given the lack of explicit exact solutions for many challenging equations, their numerical approximations provided by computers have become essential in scientific and engineering contexts [60, 64, 3, 67].

This thesis project is one of the steps contributing to these advancements. We propose novel numerical approximation methods for three SPDEs, analyze their efficiencies through mathematical and numerical analysis, and numerically illustrate their advantages.

1.1 Overview of the studied SPDEs

Here we briefly introduce the reader to the stochastic models considered in this thesis and one of their respective application areas. See Section 3 or 4 for closer details on these models. We especially recommend Sections 4.1, 4.2, 4.3, and 4.5 for physical derivations of the Schrödinger and Manakov models mentioned below.

1.1.1 The stochastic Nonlinear Schrödinger equation with white noise dispersion

A fundamental model in optics is the nonlinear Schrödinger equation (NLSE) with a power nonlinearity [97, 1, 16]. This PDE follows from considering light propagation in fiber optics, where one challenge is the chromatic dispersion of optic signals. This dispersion makes it more difficult to discern signals when using high-bit-rate transmissions, especially over long distances. It is vital to consider this dispersion to enable efficient fiber optics, such as in the Internet and other modern communication systems. Dispersion management is a multi-pronged approach, ranging from signal repeating and interpretation methods (such as wavelength division multiplexing [73]) to material engineering. The latter approach would optimally create a fiber with zero dispersion, which is a practical impossibility [14]. Instead, one proposed solution is to consider fibers with a small random dispersion that varies along the fiber and has zero average [70, 14]. We consider a model like this, termed the nonlinear Schrödinger equation with white noise dispersion (SNLSE) [70, 14, 29, 7, 22, 25].

1.1.2 The stochastic Manakov equation

The chromatic dispersion considered in the NLSE is not the only dispersion affecting light propagation. Another type of dispersion is polarization mode dispersion (PMD). The PMD follows from birefringence in the optical fibers that may vary due to (for example) core geometry, non-uniform anisotropy, or mechanical distortions from point-like pressure or twisting [39]. It is possible to model these restrictive factors as random influences leading to the Manakov PMD equation (MPMDE) and its limiting equation, the stochastic Manakov equation (SME); see [75, 15, 43] for details. The SME also serves as a model for studying long-distance light propagation in random optical fibers [68, 73].

1.1.3 The stochastic generalized Benjamin–Bona–Mahony equation

Stepping away from optics, we now consider how to model a bore in water. A bore is when the water has a steep front, meaning a sudden increase in water depth. It can also be called a positive surge or (particularly in Britain) an aegir, eagre, or eygre. Bores may form under several circumstances, taking on several characteristics, and we focus on a phenomenon called undular bores, also known as dispersed shock waves. Note that while undular bores do not only occur in water [100], we list three examples using water here: When an internal tide is propagating towards a shore, forming a hydraulic jump (or shock) which in turn disperses into an undular bore [93, 55]; in the aftermath of a tsunami, undular bores may form and in turn split up into solitary waves [48, 66]; or simply in water channels affected by the tide or gates opening and closing [81, 65].

One of the earlier works studying water wave propagation in rectangular channels led to a popular model of undular bores, the Korteweg–de Vries (KdV) equation [61]. However, the physical derivation generally requires small wave numbers and amplitudes [8], which are notable drawbacks. These issues led to the development of a substitute, the Benjamin–Bona–Mahony (BBM) equation, also known as the regularized long wave (RLW) model [81, 8, 5]. Several sources have then generalized this model in different ways. We consider two dissipative terms often presented as paired quantities [94, 99, 102, 103, 50, 49, 54], a generalized nonlinearity, and white noise dispersion [21, 35]. We call this the stochastic generalized Benjamin–Bona–Mahony equation (SBBM).

1.2 Families of numerical integrators for SPDEs

Most of the time-dependent SPDEs lack explicit, non-trivial, solutions. This problem has led to many numerical methods for approximating solutions to SPDEs. This thesis mainly considers three families of numerical methods for the time-discretization of SPDE: Euler-type, exponential, and splitting integrators. We refer the reader to Section 2.5 for more in-depth details.

Essential concepts to many physical problems are invariants [51], .i.e., properties that do not change over time. A natural question is whether preserving some or all of these invariants for a numerical integrator is possible. The difficulty of answering this question depends on the underlying problem and the approach to constructing the numerical integrator.

Euler-type integrators are the most basic type of numerical integrators. These are typically the first type of integrators a student encounters when studying ordinary differential equations, as they are comparatively easy to implement and analyze theoretically. This first venue into numerical analysis may consist of obtaining the order of the numerical scheme or even deriving what conditions are necessary for the integrator to be stable. Even in the SPDE case, though the Euler-type schemes are comparably basic, they still have their uses. Such uses include but are not limited to, being the foundation for more complicated numerical integrators designed for specific purposes.

Exponential integrators use a representation of the solution to the SPDE known as the mild solution. It allows the numerical analysis of the exponential integrators to benefit from well-explored areas such as, e.g., semigroup theory. Then, depending on the approximation of the mild solution, this may result in preserving invariants or higher order of convergence.

Splitting integrators approach the numerical approximation by decomposing the original problem into more manageable sub-problems. It is important to note that these sub-problems are only considered over each small interval as given by the time discretization. In the best cases, these sub-problems could have explicit solutions. Splitting integrators could therefore preserve invariants or have improved computational time.

1.3 The objectives and main results of the thesis

In this section we list the main objectives of this thesis, how they were achieved, and in what paper they have been achieved.

a) Perform a comprehensive numerical analysis of the SNLSE. This was done in Paper 1 by

   a_1) comparing several already existing numerical schemes,

   a_2) studying variable stepsize strategies,

   a_3) extensively investigating the blowup phenomena of solutions to the SNLSE. For more details on a conjecture regarding blowup as posed in [7], see Section 3.2.3.

b) Develop and analyze novel numerical methods for an efficient numerical integration of the SME. This was done in Paper 2 and 3 by

   b_1) developing and implementing exponential schemes (the explicit exponential integrator and symmetric exponential integrator, abbreviated EE and SE, respectively) for the SME, (Paper 2 and 3)

   b_2) developing and implementing splitting schemes for the SME, (Paper 2 and 3)

   b_3) proving the rates of convergence in the mean–square, probability, and almost surely sense of the EE for the SME, (Paper 2)

   b_4) proving the rates of convergence in the mean–square, probability, and almost surely sense of the Lie–Trotter splitting integrator, abbreviated LT, for the SME, (Paper 3)

   b_5) comparing the performance of several already existing numerical schemes. (Paper 2 and 3)

c) Study efficient numerical discretization of the SBBM. This was done in Paper 4 by

   c_1) developing, implementing, and numerically investigating the properties and convergences of exponential schemes,

   c_2) comparing the performance of several already existing numerical schemes.

d) Develop novel approach to numerically illustrate convergence in probability. See Section 2.7 for more details. (Paper 1, 3, and 4)

2

Tools and Techniques for Modeling and Simulating SPDEs

Several tools and techniques are needed to model, study, and simulate SPDEs. These include, but are not limited to, stochastic, functional, semigroup, PDE, numerical, and physical modeling theories. The theory behind SPDEs is too complicated to cover in the introduction of a thesis. Therefore we will only touch on some of the concepts necessary to understand the articles in this thesis.

While there exist approaches such as the Martingale (or Martingale measure) approach [101] and the variational (or Malliavin) calculus approach [86, 90], this thesis focuses on the semigroup (or mild solution) approach to SPDEs [27, 26, 62].

For the reader who desires more depth, we give here a few references related to a selection of the relevant areas: See [88, 96, 17, 77] for PDEs, [80, 52, 33] for semigroups, [60, 3] for SDEs, and [101, 19, 86, 27, 91] for SPDEs.

2.1 Introduction to PDE

The main reference of this section is [17]. Let us first define appropriate PDE spaces. A *measure space* is defined as the triple $(\psi, \mathcal{M}, \mu)$, where ψ is a set, $\mathcal{M}$ is a σ-algebra in ψ, and $\mu : \mathcal{M} \to [0, \infty]$ is a measure. For the purpose of this section, we restrict ourselves to $\psi \subseteq \mathbb{R}^n$, $n \in \mathbb{N}$.

Definition 2.1.1 ($\mathcal{L}^p$-space)**.** The space of all μ-integrable functions from

ψ to $\mathbb{C}$ is defined as $\mathcal{L}^1(\psi)$. For $p \in (1, \infty)$

$$\mathcal{L}^p(\psi) = \left\{ f : \psi \to \mathbb{C}; f \text{ measurable } ; |f|^p \in \mathcal{L}^1(\psi) \right\}.$$

For $p = \infty$

$$\begin{aligned} \mathcal{L}^\infty(\psi) = \{ & f : \psi \to \mathbb{C}; f \text{ measurable } ; \\ & f \text{ bounded } \mu\text{-almost everywhere (a.e.) on } \psi \}. \end{aligned}$$

The corresponding seminorms are defined as

$$\|f\|_{\mathcal{L}^p(\psi)} = \left[\int_\psi |f(x)|^p \, \mathrm{d}\mu(x) \right]^{1/p}$$

for $p \in [1, \infty)$ and

$$\|f\|_{\mathcal{L}^\infty(\psi)} = \inf\{C; |f(x)| \leqslant C \ \mu\text{-a.e. on } \psi\}.$$

for $p = \infty$.

These seminorms cannot distinguish functions that are equal μ-almost everywhere, and therefore we define, for some $p \in [0, \infty]$,

$$\mathcal{N} = \{ f \in \mathcal{L}^p(\psi) : \|f\|_{\mathcal{L}^p(\psi)} = 0 \}.$$

We then consider the *coset* of $f \in \mathcal{L}^p(\psi)$,

$$f + \mathcal{N} := \{ f + g : g \in \mathcal{N} \}.$$

This gives us the quotient vector space induced by the above seminorms.

Definition 2.1.2 (L^p-space)**.** For $p \in [0, \infty]$, the quotient space $\mathcal{L}^p(\psi)/\mathcal{N}$ is defined as the set of cosets

$$L^p(\psi) = \{ f + \mathcal{N} : f \in \mathcal{L}^p(\psi) \}.$$

It is clear that, for $f \in \mathcal{L}^p(\psi)$, $p \in [0, \infty]$, the set

$$\left\{ \|f + g\|_{\mathcal{L}^p(\psi)} : g \in \mathcal{N} \right\}$$

contains only one element, and we denote this element as $\|f\|_{L^p(\psi)}$. The induced norm can then be written as

$$\|f + \mathcal{N}\|_{L^p(\psi)} := \|f\|_{L^p(\psi)} = \|f\|_{\mathcal{L}^p(\psi)}.$$

In fact, see the Riesz–Fischer Theorem [17, page 93], for $p \in [1, \infty]$ we have that L^p is a complete vector space, also known as a *Banach space*. For the special case of $p = 2$ we also find that L^2 is a Hilbert space, with the inner product

$$\langle f, g \rangle_{L^2(\psi)} = \int_\psi f(x)\overline{g(x)}\mathrm{d}\mu(x).$$

To simplify the notation, we write mixed partial derivatives in dimension $n = \dim(\psi)$. Then, for $\alpha \in \mathbb{N}^n$ and $|\alpha| = \alpha_1 + \alpha_2 + \ldots \alpha_n$, we introduce the multi-index notation

$$D^\alpha = \frac{\partial^{|\alpha|}}{\partial_{x_1}^{\alpha_1} \partial_{x_2}^{\alpha_2} \ldots \partial_{x_n}^{\alpha_n}}.$$

This allows us to concisely give the following definition.

Definition 2.1.3 (Sobolev space)**.** Let $p \in [0, \infty]$ and $m \in \mathbb{N}$. The **Sobolev space** $W^{m,p}(\psi)$ is defined as

$$W^{m,p}(\psi) = \{f \in L^p(\psi); D^\alpha f \in L^p(\psi) \quad \forall |\alpha| \leqslant m\},$$

where the derivatives are interpreted in the weak sense.

The corresponding Sobolev norm is then

$$\|f\|_{W^{m,p}(\psi)} = \begin{cases} \left(\sum_{|\alpha| \leqslant m} \|D^\alpha f\|_{L^p(\psi)}^p\right)^{1/p}, & p \in [1, \infty) \\ \max_{|\alpha| \leqslant m} \|D^\alpha f\|_{L^\infty(\psi)}, & p = \infty. \end{cases}$$

As with L^2 we have the special case for $p = 2$, with the notation $H^m(\psi) := W^{m,2}(\psi)$. It has the corresponding inner product

$$\langle f, g \rangle_{H^m(\psi)} = \sum_{\alpha=0}^{m} \sum_{|\beta|=\alpha} \int_\psi (D^\beta f)\overline{(D^\beta g)}\mathrm{d}\mu,$$

where the sum over β is the sum over all multi-indexes such that $|\beta| = \beta_1 + \beta_2 + \ldots + \beta_n = \alpha$.

2.1.1 Semigroup theory & types of solutions

In general, a semigroup is a set with a binary operation defined on it, such that the binary operation is associative. If we then consider a semigroup of operators on a Hilbert space H, $\{S(t) : H \to H; t \geqslant 0\}$, we call it a C_0-semigroup on H if

1. $S(0) = I$ and $S(t+h) = S(t)S(h)$ for all $t, h \geqslant 0$,

2. $\lim_{h \to 0^+} S(h)X = X$ for all $X \in H$.

This semigroup can then be linearized to give the infinitesmal generator of the semigroup, which is the linear operator L defined according to

$$LX := \lim_{h \to 0^+} \frac{S(h)X - X}{h}$$

for all $X \in H$ where the above limit exists.

Let us inspect a model problem

$$\begin{cases} X'(t) = LX(t) + f(t) \\ X(0) = X_0 \end{cases} \tag{2.1}$$

where $t \in [0, T]$, $X_0 \in H$, $f \in L^1([0, T])$, and L is the infinitesimal generator for some analytic C_0-semigroup $\{S(t) : H \to H; t \geqslant 0\}$. For closer details on what it means for a semigroup to be analytic, see for instance [33]. With this, we have two types of solutions.

Definition 2.1.4 (Strong solution)**.** A function $X : [0, T] \to H$ which

- is differentiable almost everywhere on $[0, T]$,
- has $X' \in L^1([0, T] \times H)$,
- has $X(0) = X_0$, and
- $X'(t) = LX(t) + f(t)$ almost everywhere on $t \in [0, T]$

is called the **strong solution** to Equation (2.1).

Definition 2.1.5 (Mild solution)**.** A function $X : [0, T] \to H$ defined according to

$$X(t) := S(t)X_0 + \int_0^t S(t-s)f(s)\mathrm{d}s,$$

fulfilling

$$\sup_{t \in [0,T]} \|X(t)\|_H^2 < \infty,$$

is called the **mild solution** to Equation (2.1).

2.2 Brief overview of stochastic analysis

We stress again that for additional depth or details, we refer to, e.g., [86]. Let $(\Omega, \mathcal{A}, \mathbb{P})$ denote a probability space. We equip it with a filtration $\mathcal{F} = \{\mathcal{F}_t, t \in \mathbb{T}\}$ for some index set $\mathbb{T}$. This filtration satisfies, as is usual, the following conditions

1. $\mathcal{F}_0$ contains all $\mathbb{P}$-null sets of $\mathcal{A}$.
2. $\mathcal{F}$ is right-continuous. That is,

$$\mathcal{F}_t = \bigcap_{s>t} \mathcal{F}_s$$

for all $t, s \in \mathbb{T}$.

This allows us to define the core concept of SPDEs.

Definition 2.2.1 (Random variable in Hilbert space)**.** Let H be a Hilbert space, and let $\mathcal{B}(H)$ be the Borel σ-algebra on H. Then a measurable function $X : (\Omega, \mathcal{A}) \to (H, \mathcal{B}(H))$ is a **H-valued random variable**.

The definition of stochastic processes naturally follows.

Definition 2.2.2 (Stochastic process)**.** A set of random variables $R = \{X(t)\}_{t\in\mathbb{T}}$, for some index set $\mathbb{T}$, is a **stochastic process**. If, for all $t \in \mathbb{T}$, $X(t)$ are H-valued random variables we say that R is a **H-valued stochastic process**.

Commonly $\mathbb{T}$ is the set of non-negative real numbers, an interval of the form $[a, b]$, or non-negative integers. In this thesis, we consider $\mathbb{T} = [0, T]$ for some $T > 0$, or $\mathbb{T} = \mathbb{R}^+$.

One of the stochastic processes considered in the articles in this thesis is the well-known Wiener process.

Definition 2.2.3 (Wiener process)**.** A stochastic process $W : \Omega \times \mathbb{R}^+ \to \mathbb{R}$ is called a **standard Wiener process** if

1. $W(0) = 0$ almost surely.
2. The sample paths of W are continuous over $\mathbb{R}^+$ almost surely.
3. W has independent increments. I.e. for all $(s_1, t_1), (s_2, t_2) \subset \mathbb{R}^+$, $W(t_1) - W(s_1)$ is independent of $W(t_2) - W(s_2)$ if $(s_1, t_1) \cap (s_2, t_2) = \varnothing$.

4. $W(t) - W(s) \sim N(0, t-s)\ \forall t \geqslant s$. I.e. the increments are normally distributed with mean 0 and variance equal to the increment interval length.

One of the properties of the Wiener process is that, while it is almost surely continuous over $\mathbb{R}^+$, it is also almost surely non-differentiable over $\mathbb{R}^+$.

Much like the stochastic integrals for SDEs, the formal path to constructing stochastic integrals for SPDEs begins by constructing H-valued elementary processes. To simplify the notation, we first define the following.

Definition 2.2.4 (Indicator function)**.** For some set A, the function

$$I_A(t) = \begin{cases} 1, & t \in A, \\ 0, & \text{elsewhere.} \end{cases}$$

is called the **indicator function**.

We can now split up our index set and define the following elementary processes accordingly.

Definition 2.2.5 (H-valued elementary process)**.** Take the index set $\mathbb{T}$ and some finite partition $\{[t_i, t_{i+1})\}_{i=1}^N = \{\mathbb{T}_i\}_{i=1}^N$, with $t_{N+1} = \infty$ if $\mathbb{T} = \mathbb{R}^+$. We say that an H-valued stochastic process X is an **H-valued elementary process** if

$$X(t) = \sum_{i=0}^{N} X_i I_{\mathbb{T}_i}(t),$$

for some set of H-valued random variables $\{X_i\}_{i=0}^N$. We use $\mathbb{H}$ to denote the set of H-valued elementary processes.

The stochastic integrals with respect to these elementary processes are defined as follows.

Definition 2.2.6 (Stochastic integrals of H-valued elementary process)**.** Take the Wiener process W, and an H-valued elementary process X with the partition of the interval $[a, b)$ according to $\{[t_i, t_{i+1})\}_{i=0}^N$. Then the **Itô stochastic integral** of X over $[a, b]$ is defined as

$$\int_a^b X(t) \mathrm{d}W = \sum_{i=0}^{N-1} X_i (W(t_{i+1}) - W(t_i)).$$

The **Stratonovich stochastic integral** of X over $[a,b]$ is defined as

$$\int_a^b X(t) \circ \mathrm{d}W = \sum_{i=0}^{N-1} \left(\frac{X_i + X_{i+1}}{2} \right) (W(t_{i+1}) - W(t_i)).$$

The symbol $\circ$ is known as the Stratonovich product.

By constructing a sequence of processes in $\mathbb{H}$, $\{X_i\}_{i=1}^{\infty}$ that converges towards some H-valued stochastic process X in the completion of $\mathbb{H}$, denoted $\bar{\mathbb{H}}$, we get the following definition.

Definition 2.2.7 (Stochastic integral of H-valued stochastic processes)**.** Take a sequence $\{X_i\}_{i=1}^{\infty}$, $X_i \in \mathbb{H}$ $\forall i \geqslant 1$ such that $X = \lim_{i\to\infty} X_i \in \bar{\mathbb{H}}$. Then the **Itô stochastic integral** of X over $[a,b]$ is defined as

$$\int_a^b X(t)\mathrm{d}W = \lim_{i\to\infty} \int_a^b X_i(t)\mathrm{d}W$$

and the **Stratonovich stochastic integral** of X over $[a,b]$ is defined as

$$\int_a^b X(t) \circ \mathrm{d}W = \lim_{i\to\infty} \int_a^b X_i(t) \circ \mathrm{d}W.$$

Remark 2.2.8. Observe that the values of the Itô and Stratonovich integrals are not dependent of the choice of sequences $\{X_i\}_{i=1}^{\infty}$.

Remark 2.2.9. The limits of these integrals are interpreted in the mean–square sense,

$$\lim_{i\to\infty} X_i = X \Leftrightarrow \lim_{i\to\infty} E\left[\|X_i - X\|_H^2 \right] = 0.$$

2.3 The Monte Carlo method

The Monte Carlo method is a powerful statistical technique that leverages random sampling to estimate various underlying properties or a random variable, e.g. $\|X(t)\|_{L^2}$, including the mean, probability of events, and variance [89]. Take a set of independent and identically distributed real-valued random variables $\{X_n\}_{n=1}^{N}$ for a given $N = 2, 3, \ldots$. With this set of random variables, we can calculate the sample mean $\bar{X}$ and sample standard deviation $s(X)$ using the formulas:

$$\bar{X} = \frac{1}{N} \sum_{n=1}^{N} X_n, \quad s(X) = \sqrt{\frac{1}{N-1} \sum_{n=1}^{N} (X_n - \bar{X})^2}.$$

When using the Monte Carlo method, choosing an appropriate sample size that balances the accuracy of the estimates and the computational resources required is crucial. This balance becomes especially important when comparing two sample means, such as when estimating weak errors. The difference between the estimates would have to be greater than the Monte Carlo error, which is defined as the standard deviation of the sample mean,

$$\sqrt{V\left[\bar{X}\right]} = \sqrt{V\left[\frac{1}{N}\sum_{n=1}^{N} X_n\right]} = \frac{1}{\sqrt{N}}\sqrt{V\left[X_1\right]}.$$

Remark 2.3.1. Observe that the sample mean, $\bar{X}$, and sample standard deviation, $s(X)$, are both random variables.

2.4 Spatial discretization of PDEs

Here we give a brief rundown of the two methods of spatial discretization used in the articles included in this thesis: The finite difference method [77] and the pseudospectral method [46]. Naturally, there are a number of other methods to discretize (S)PDEs in space, such as the finite element method [63] (usually denoted FEM) or the finite volume method [31] (usually denoted FVM).

In order to keep the explanations of the spatial discretization methods brief, we limit ourselves to the function $X : \mathbb{R}^+ \times [a, b] \to \mathbb{R}$ obeying the PDE

$$\frac{\partial}{\partial t}X + \frac{\partial}{\partial x}X + \frac{\partial^2}{\partial x^2}X + f(X) = 0, \tag{2.2}$$

where $f : \mathbb{R} \to \mathbb{R}$ is some nonlinear function. We use Dirischlet homogeneous boundary conditions for the finite difference method, $X(a) = X(b) = 0$, and periodic boundary conditions for the pseudo-spectral method, $X(a) = X(b)$.

2.4.1 The finite difference method (FD)

We will assume homogeneous Dirichlet boundary conditions. Take an integer $M \geqslant 1$ and define the mesh of the finite difference discretization by $\Delta x = (b - a)/M$. Furthermore, we denote a discrete grid by $x_m = a + m\Delta x$, for $m = 0, 1, \ldots, M$. A centered finite difference approximation of Equation (2.2) then results in the following system

$$\frac{\partial}{\partial t}X^m + \frac{X^{m+1} - X^{m-1}}{2\Delta x} + \frac{X^{m+1} - 2X^m + X^{m-1}}{(\Delta x)^2} + f(X^m) = 0, \tag{2.3}$$

where $X^m : \mathbb{R}^+ \to \mathbb{R}$, $X^0 = X^M = 0$, and $m = 0, 1, \ldots, M$. One then gets the numerical approximation $X^m \approx X(\cdot, x_m)$.

2.4.2 The pseudospectral method (PS)

We will assume periodic boundary conditions. The pseudospectral method represents the solution as a sum of Fourier modes, computing the spatial derivatives using the Fourier transform. This method may be more time-efficient than the FD method, particularly when considering smooth functions and efficient use of the fast Fourier transform. Using the M Fourier modes of X, one obtains the semi-discrete problem

$$\frac{\partial}{\partial t} X^m + i m^* X^m - (m^*)^2 X^m + f(X)^m = 0, \tag{2.4}$$

where $X^m : \mathbb{R}^+ \to \mathbb{R}$ is the m'th Fourier mode of X, $m^* = \frac{2\pi}{b-a} m$, $f(X)^m$ is the m'th Fourier mode of $f(X)$, and $m = 1, 2, \ldots, M$.

2.5 Commonly used time integrators

As with the spatial discretization, there are several approaches to discretizing (S)PDEs in time. To describe the main ideas behind the Euler-type, exponential, and splitting integrators, take a H-valued stochastic process X which obeys the SPDE

$$\begin{aligned} \mathrm{d}X(t) &= (AX(t) + F(X(t)))\mathrm{d}t + BX(t) \circ \mathrm{d}W(t) && (2.5) \\ &= (L(t)X(t) + F(X(t)))\mathrm{d}t && (2.6) \\ X(0) &= X_0 \end{aligned}$$

where $X_0 \in H$, W is the Wiener process, A, B are linear operators, $F : H \to H$ is a nonlinear function, and $L(t)$ is the generator of a stochastic flow $S(t, s) : H \to H$, for $s < t$. This SPDE has the corresponding (for more formal details, we refer the reader to e.g. [20, 62, 70, 22, 12]) mild solution

$$X(t) = S(t, 0)X_0 + \int_0^t S(t, s)F(X(s))\mathrm{d}s. \tag{2.7}$$

Going forward, we consider a time step size $h > 0$ and the resulting uniform partition $I_N = \{t_n\}_{n=0}^{\infty} = \{hn\}_{n=0}^{\infty}$ of $\mathbb{T} = \mathbb{R}^+$. We also use half-steps, which we denote as $t_{n+1/2} = t_n + h/2$, and partition the Wiener process W accordingly, denoting the increments as $\Delta W_n = W(t_{n+1}) - W(t_n)$.

Accompanying each definition, we also introduce their corresponding notation used throughout this thesis.

2.5.1 Euler-type integrators

The formulation of Equation (2.5) is the starting point to derive the Euler-type integrators.

Definition 2.5.1 (Midpoint integrator)**.** For an initial value $X_0 \in H$, the **midpoint integrator**, denoted MP, is defined as

$$X_{n+1} = X_n + hA\left(\frac{X_n + X_{n+1}}{2}\right) + hF\left(\frac{X_n + X_{n+1}}{2}\right) + \Delta W_n B\left(\frac{X_n + X_{n+1}}{2}\right).$$

Resembling the midpoint integrator, the following integrator is very popular.

Definition 2.5.2 (Crank–Nicolson integrator)**.** For an initial value $X_0 \in H$ the **Crank–Nicolson integrator**, denoted CN, is defined as

$$X_{n+1} = X_n + hA\left(\frac{X_n + X_{n+1}}{2}\right) + h\frac{F(X_n) + F(X_{n+1})}{2} + \Delta W_n B\left(\frac{X_n + X_{n+1}}{2}\right).$$

Remark 2.5.3. Observe that it is common to approximate F in the CN, leading to many variations, see e.g. [7].

2.5.2 Exponential integrators

The mild solution, Equation (2.7), is the starting point to derive the exponential integrators. We begin by approximating the integral using an Euler approximation.

Definition 2.5.4 (θ-exponential integrator)**.** For an initial value $X_0 \in H$ and $\theta \in [0, 1]$, we have that the **θ-exponential integrator** is defined as

$$X_{n+1} = S(t_{n+1}, t_n)\left(X_n + hF\left(\theta X_n + (1-\theta)X_{n+1}\right)\right).$$

For $\theta = 1, 0.5, 0$ one obtains the **explicit**, **midpoint**, and **backward exponential integrators** respectively. They are, in order, denoted EE, ME, and BE.

This approach can be refined further by introducing a symplectic, or symmetric, variant [20].

Definition 2.5.5 (Symmetric exponential integrator)**.** For an initial value $X_0 \in H$ the **symmetric exponential integrator**, denoted SE, is defined as

$$\begin{aligned} X_* &= F\left(S\left(t_{n+1/2}, t_n\right) X_n + \frac{h}{2} X_*\right) \\ X_{n+1} &= S(t_{n+1}, t_n) X_n + hS\left(t_{n+1}, t_{n+1/2}\right) X_*. \end{aligned}$$

In the articles considered in this thesis, the symmetric exponential integrator displays several advantageous qualities, including preserving quadratic invariants or even displaying a higher order of convergence (depending on the model, see [10]).

2.5.3 Splitting integrators

The formulation of Equation (2.6) is the starting point to derive the splitting integrators. See, e.g., [51] for splitting integrators applied to SDEs. For two finite partitions of the step $[t_n, t_{n+1}]$, one for the linear and one for the nonlinear part, respectively, splitting integrators alternates between the flows of these parts, respecting said partitions. In practice, the implementation of these steps may overlap with the flow as found in the mild solution or even use explicit solutions. Therefore we will use the notation S for the linear flow. Correspondingly, we use Z to denote the nonlinear flow. That is, for the flow of the nonlinear part

$$X'(t) = F(X(t)),$$

over the time increment $[t_n, t_{n+1}]$, with initial value X_n, we write $Z(t_n, h)X_n$. We can now define two of the more famous splitting integrators.

Definition 2.5.6 (Lie–Trotter splitting integrator)**.** For an initial value $X_0 \in H$ the **Lie–Trotter splitting integrator**, denoted LT, is defined as

$$\begin{aligned} X_{n+1/2} &= S(t_n, h)X_n \\ X_{n+1} &= Z(t_n, h)X_{n+1/2}. \end{aligned}$$

Definition 2.5.7 (Strang splitting integrator)**.** For an initial value $X_0 \in H$ the **Strang splitting integrator**, denoted ST, is defined as

$$\begin{aligned} X_{n+1/2} &= S(t_n, h/2)X_n \\ X_* &= Z(t_n, h)X_{n+1/2} \\ X_{n+1} &= S(t_{n+1/2}, h/2)X_*. \end{aligned}$$

2.6 Some types of stochastic convergences

Naturally, given a numerical approximation of a solution to some SPDE, we are interested in three things: Whether the numerical approximation converges toward the exact solution; for what norm it converges; and with what order (speed). With the introduction of stochasticity to PDEs we need to adapt the types of convergence. We introduce a selection of them here, and refer the curious reader to e.g. [60, 3] for more details.

In order to simplify the notation slightly, we will consider samples $\omega \in \Omega$, time $t \in \mathbb{T} = [0, T]$, and spatial coordinates $x \in \mathbb{R}$. Then for some SPDE with solution X we discretize in time using the uniform partition $I_N(T) = \{t_n\}_{n=0}^N = \{hn\}_{n=0}^N$ of $\mathbb{T}$ for some $N \in \mathbb{Z}^+$ and time step size $h = T/N$. The numerical approximation of X at t_n is denoted by $X_n(x, \omega) \approx X(t_n, x, \omega)$, $n = 0, 1, \ldots, N$ and we denote the error for a given norm $\mathcal{N}$ with

$$e(T, N, \mathcal{N}, \omega) = \max_{t_n \in I_N(T)} \|X_n(\cdot, \omega) - X(t_n, \cdot, \omega)\|_{\mathcal{N}}.$$

We say that a numerical scheme converges (with order $\delta > 0$ and with respect to the norm $\mathcal{N}$)

- **In mean–square** (or strongly) if there exists a constant C, not dependent on N, such that for all N big enough,

$$\sqrt{\mathbb{E}\left[e(T, N, \mathcal{N}, \cdot)^2\right]} \leqslant Ch^\delta. \tag{2.8}$$

- **In probability** if for all $h \leqslant 1$

$$\lim_{C \to \infty} \mathbb{P}\left(e(T, N, \mathcal{N}, \cdot) \geqslant Ch^\delta\right) = 0, \tag{2.9}$$

  or, equivalently, if for any $\varepsilon \in (0, 1]$ there exists a $C(\varepsilon) \in \mathbb{R}$ s.t. for any $h \leqslant 1$

$$\mathbb{P}\left(e(T, N, \mathcal{N}, \cdot) \geqslant C(\varepsilon)h^\delta\right) < \varepsilon. \tag{2.10}$$

- **Almost surely** if for all $\hat{\delta} \in (0, \delta)$, there exists a random variable $K_{\hat{\delta}}(T, \omega)$ such that

$$e(T, N, \mathcal{N}, \omega) \leqslant K_{\hat{\delta}}(T, \omega) h^{\hat{\delta}} \qquad \mathbb{P} - a.s.,$$

  for N sufficiently large.

- **Weakly** if for any functional ϕ (of a nice enough class of functionals), there exists a constant $C(\phi)$ such that, for N big enough,

$$\max_{t_n \in I_N(T)} |\mathbb{E}\left[\phi(X_n)\right] - \mathbb{E}\left[\phi(X(t_n, \omega))\right]| \leqslant C(\phi) h^{\delta}.$$

We want to stress that the weak convergence does not use the norm $\mathcal{N}$. Further, since the weak errors compare two means, it is important to ensure that the Monte Carlo error does not overshadow their differences and that special considerations are taken.

2.7 Methods for illustrating convergences numerically

A numerical investigation into how a numerical integrator converges will be limited, given that a computer has a finite time to perform its calculations. This limitation primarily displays itself in a finite selection of time step sizes h chosen to illustrate the convergence of interest. A reference solution often replaces the exact solution X due to a lack of explicit solutions, and it uses a time step size smaller than the selected h considered. Aside from the choice of time step sizes, it is also important to remember that the estimations of the means and probabilities are heavily dependent on the sample sizes. As an example of how the distribution of the errors looks in the standard and logarithmic perspectives, we present Figure 2.1. To be clear: We also illustrate some numerical cumulative distribution functions (CDFs) in the logarithmic perspective, e.g., Figure 2.3.

Any illustration in this section will display actual data simulated for the SBBM, with a total of 600 samples. We introduce the notation across the following subsections: The sample size is denoted $B > 0$, and the individual samples will be denoted $\omega_i \in \Omega$, $i = 1, 2, \ldots, B$.

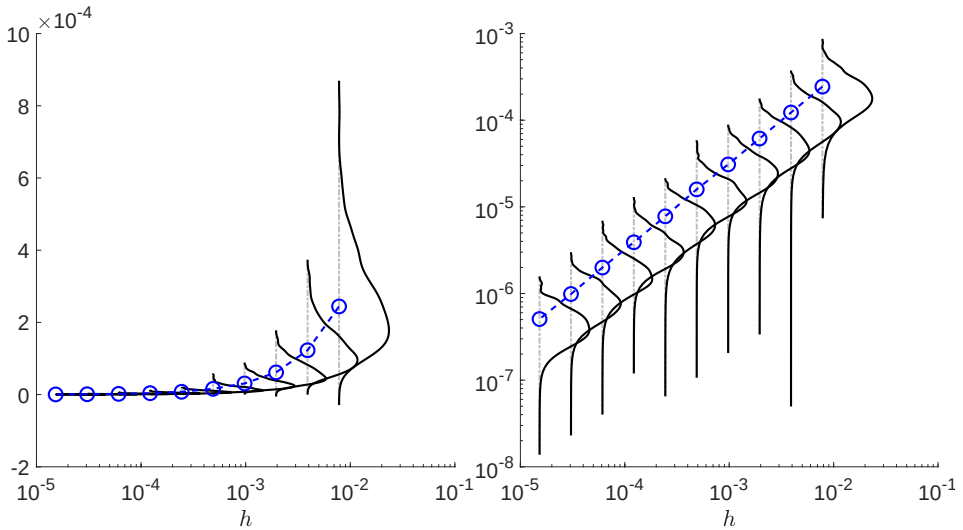

Figure 2.1: Smoothed distributions of $\mathbb{H}^1$-norm errors of the SE for the SBBM, at given time step sizes h, with the means of the errors marked using blue circles. Semi-log plot to the left, log-log plot to the right.

2.7.1 Mean–square and weak convergence

When it comes to illustrating the accuracy of a numerical scheme, the most common method is to numerically illustrate the strong or weak orders of convergence. The method of illustrating the order of mean–square convergence is as follows. Defining

$$\mathrm{err}(T/N) = \mathrm{err}(h) = \mathbb{E}\left[e(T, N, \mathcal{N}, \omega)\right]$$

and taking the logarithm of Equation (2.8) yields

$$\log \mathrm{err}(h) \leqslant \log(C) + \delta \log(h).$$

We recognize the right-hand side as the equation of a line with intercept $\log(C)$ and slope δ. We compare $\log \mathrm{err}(h)$ to this line. We can therefore display the mean–square order of convergence for a number of numerical schemes simultaneously and compactly, as seen in Figure 2.2 which contains the corresponding Monte Carlo estimates of $\mathrm{err}(h)$.

Illustrating the order of weak convergence is visually identical, with the only caveat that the sample sizes often have to be much larger due to the Monte Carlo error, see Section 2.3.

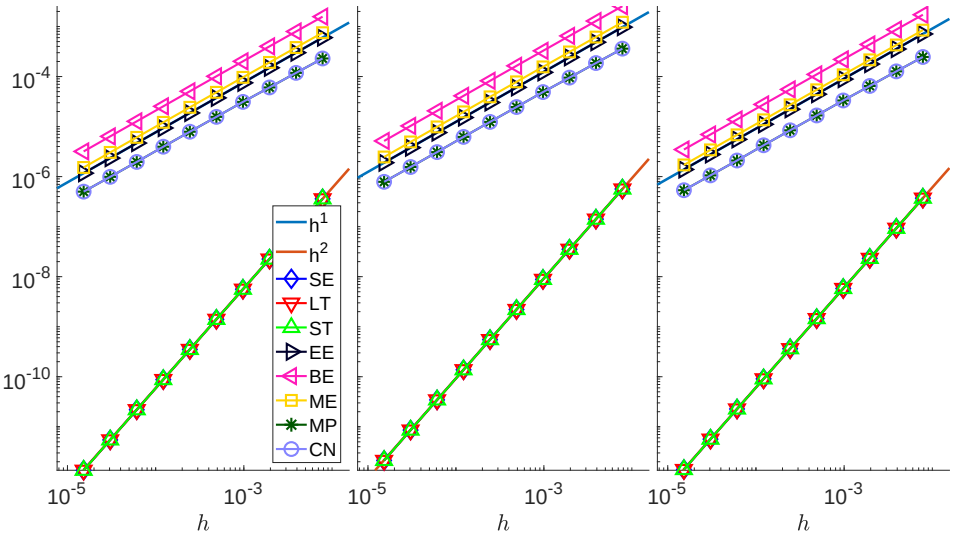

Figure 2.2: An illustration of the strong, or mean–square, convergence rates. Evaluation of the linear SBBM using three different norms, $\mathbb{L}^2$-norm left, $\mathbb{H}^1$-norm middle, $\mathbb{L}^\infty$-norm right.

2.7.2 Convergence in probability

As seen in the definition of convergence in probability, we have two perspectives we can approach from. In the following illustrations we will make use of data obtained from numerical experiments simulating the SBBM, as performed in [10].

Starting with Equation (2.9) we can approximate the probability $\mathbb{P}$ with the proportion of samples fulfilling the same criteria. For some $C > 0$, let

$$A(C) = A(T, N, \mathcal{N}, C) = \left\{\omega \in \Omega : e(T, N, \mathcal{N}, \omega) \geqslant Ch^\delta\right\}.$$

Then

$$P(h, \mathcal{N}, C, \delta, B) := \frac{\sum_{i=1}^{B} I_{A(C)}(\omega_i)}{B} \approx \mathbb{P}\left(e(T, N, \mathcal{N}, \omega) \geqslant Ch^\delta\right)$$

for some large sample size B and $h = T/N$. We observe how this fraction behaves as $h \to 0$ and $C \to \infty$. We want to capture the behavior of P for a range of C using the chosen h given a hypothesized order of convergence δ. This method is denoted as the P-estimation method.

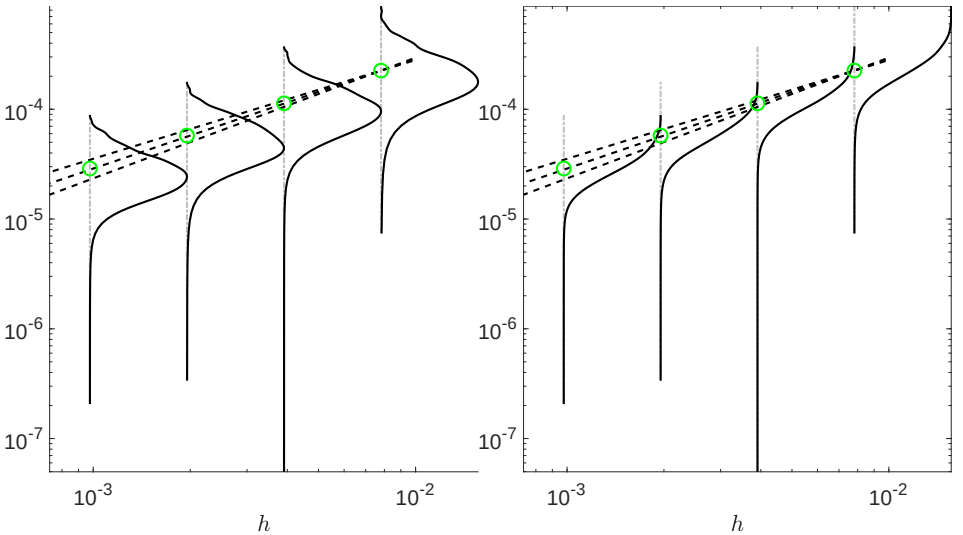

Figure 2.3: Smoothed distributions of $\mathbb{H}^1$-norm errors of the SE for the SBBM, at given time step sizes h, with the median marked using green circles. Distribution plot to the left, CDF plot to the right. The three dashed lines are $C_\delta h^\delta$, $\delta = 0.9, 1, 1.1$.

A first attempt to visualize the P-estimation method can be seen in [4, p. IV:19] and an improvement was then made in [11]. As an aide of understanding the behavior of P, we use Figure 2.3. We use three lines $C_\delta h^\delta$ for $\delta = 0.9, 1, 1.1$ and have chosen C_δ such that the lines intersect at the median of the errors for the greatest step-size. We see how $P(h, \mathbb{H}^1, C_\delta, \delta, 600)$, as a function of $N = T/h$, decreases for $\delta = 0.9$, stays approximately the same for $\delta = 1$, and increases for $\delta = 1.1$ as $h \to 0$. This is illustrative of the behavior for the order of convergence in probability, which in this case is $\delta = 1$. To ensure consistency, this behavior of P can then be observed over a larger set of values for C and $h = T/N$, as seen in Figure 2.4.

The second perspective of illustrating convergence in probability, Equation (2.10), relies on estimating the translation coefficient $C(\varepsilon)$ for $\varepsilon \in \{1/B, 2/B, \ldots, B/B\}$. This method is denoted as the C-estimation method. A first attempt at illustrating the rate of convergence in probability using the C-estimation method can be seen in [11]. Define

$$C(h, \mathcal{N}, \varepsilon, \delta, B) = \inf \left\{ C \in \mathbb{R}^+ : P(h, \mathcal{N}, C, \delta, B) \geqslant \varepsilon \right\}.$$

Taking fixed B, $\mathcal{N}$, and set of time step sizes h, then for each δ we get a

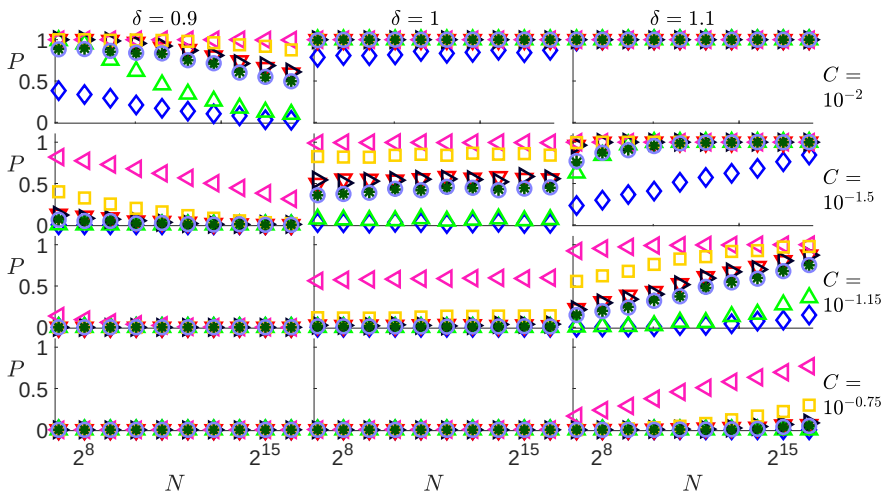

Figure 2.4: Using the P-estimation method, an illustration of the convergence in probability of 8 numerical schemes for the SBBM equation, in the $\mathbb{L}^2$-norm.

range of $C(h, \mathcal{N}, \varepsilon, \delta, B)$ spanning our set of h. For the sake of visualization, these C estimations are then normalized via

$$\tilde{C}(\delta, h, \varepsilon, \mathcal{N}, B) = \frac{C(h, \mathcal{N}, \varepsilon, \delta, B)}{\sup_{\hat{h}} C(\hat{h}, \mathcal{N}, 1/B, \delta, B)}$$

forcing $\tilde{C}$ for the lowest percentile to be 1, i.e. $\sup_h \tilde{C}(\delta, h, 1/B, \mathcal{N}, B) = 1$. As an illustration, we have estimated $C(h, \mathbb{H}^1, 0.5, \delta, 600)$ for $\delta \in \{0.9, 1, 1.1\}$ and a selection of a few time step sizes in Figure 2.5. We observe how the span of the translation coefficient is the smallest for $\delta = 1$. This means that for a nice enough choice of set of time step sizes we expect that the range of $\tilde{C}$ is minimized for the correct order of convergence δ. We can see $\tilde{C}(\delta, h, \varepsilon, \mathbb{H}^1, 600)$ ranges obtained by the SE for the SBBM in Figure 2.6.

The downside of the C-estimation method, as seen in Figure 2.6, is the lack of density: with one numerical scheme occupying an entire figure. A natural next step, as considered in [10], would be to consider the integral of the ranges obtained by the C-estimation method.

By imposing a few harsh assumptions on the distribution of the errors we get the beginnings of the $I(\delta)$-estimation method.

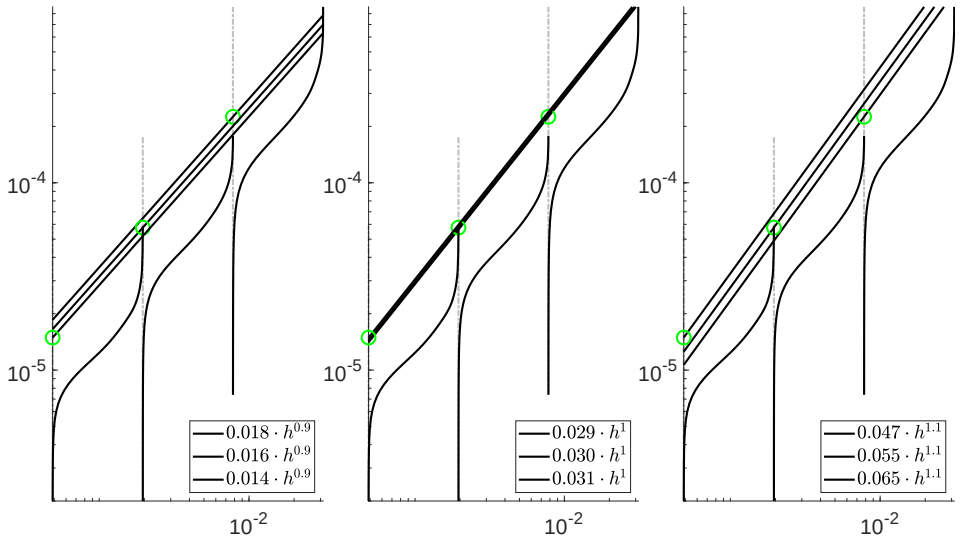

Figure 2.5: Smoothed distributions of $\mathbb{H}^1$-norm errors of the SE for the SBBM, at given time step sizes h, with the median marked using green circles. Each CDF is plotted with three lines $C_h h^\delta$, ($\delta = 0.9, 1, 1.1$ in the left, middle, and right plots respectively), where C_h is chosen such that the line intersects the median of the errors for time step size h.

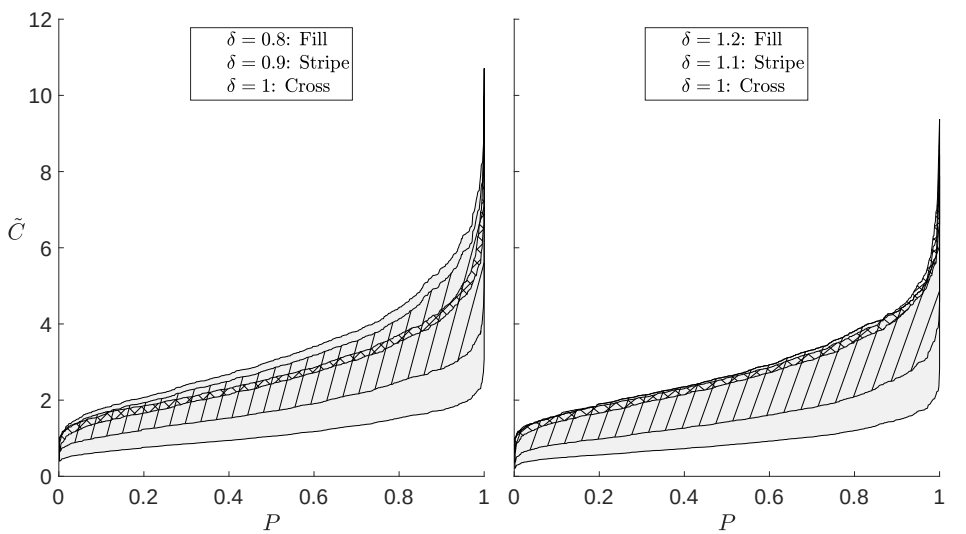

Figure 2.6: Using the C-estimation method, an illustration of the convergence in probability of SE for the SBBM equation, in the $\mathbb{H}^1$-norm.

Proposition 2.7.1. *Consider a numerical scheme with numerical errors $e(T, N, \mathcal{N}, \cdot)$ for a norm $\mathcal{N}$. If there exists some upper limit $\hat{h} > 0$ such that $\forall h = T/N < \hat{h}$ there exists a strictly monotonic continuous CDF $F_h : \mathbb{R}^+ \to [0, 1]$ for the numerical errors $e(T, N, \mathcal{N}, \cdot)$, and*

$$I(\delta) := \int_0^1 \sup_{h \in (0, \hat{h}]} \frac{F_h^{-1}(\varepsilon)}{h^\delta} - \inf_{h \in (0, \hat{h}]} \frac{F_h^{-1}(\varepsilon)}{h^\delta} \mathrm{d}\varepsilon = 0,$$

then this numerical scheme converges in probability with order δ with respect to $\mathcal{N}$.

Proof. Since F_h, for any given $h \in (0, \hat{h}]$, is strictly monotonic and continuous, we have that the corresponding quantile function F_h^{-1} is continuous. This means that $I(\delta)$ is an integral of a continuous non-negative function. Combined with $I(\delta) = 0$ we can therefore conclude that, for all $\varepsilon \in (0, 1)$,

$$\sup_{h \in (0, \hat{h}]} \frac{F_h^{-1}(\varepsilon)}{h^\delta} = \inf_{h \in (0, \hat{h}]} \frac{F_h^{-1}(\varepsilon)}{h^\delta}.$$

This means that

$$\frac{F_{h_1}^{-1}(\varepsilon)}{h_1^\delta} = \frac{F_{h_2}^{-1}(\varepsilon)}{h_2^\delta}, \quad \forall h_1, h_2 \in (0, \hat{h}],$$

or, equivalently, that

$$F_h^{-1}(\varepsilon) = F^{-1}(\varepsilon) h^\delta, \quad \forall h \in (0, \hat{h}]$$

for some CDF F. We can rewrite this according to

$$\varepsilon = F_h(F^{-1}(\varepsilon) h^\delta).$$

If we then choose $C(\varepsilon) = F^{-1}(1 - \varepsilon/2)$ for any given $\varepsilon > 0$, we have that

$$\begin{aligned} P(e(T, N, \mathcal{N}, \cdot) \geqslant C(\varepsilon) h^\delta) &= 1 - F_h(C(\varepsilon) h^\delta) \\ &= 1 - F_h(F^{-1}(1 - \varepsilon/2) h^\delta) = \varepsilon/2 < \varepsilon, \end{aligned}$$

and we therefore have convergence in probability with order δ. □

Using the experimental data, we have estimated $I(\delta)$ in Figure 2.7. The shape of the curves is due to the factor

$$|h_{max}^{\hat{\delta}-\delta} - h_{min}^{\hat{\delta}-\delta}| = |h_{max}^{-a} - h_{min}^{-a}|,$$

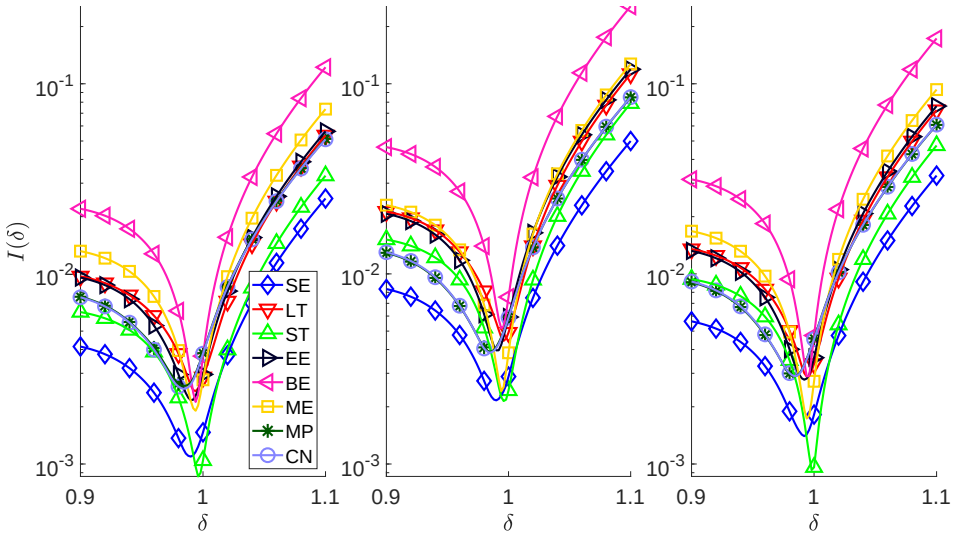

Figure 2.7: Using the $I(\delta)$-estimation method, an illustration of the convergence in probability of 8 numerical schemes for the SBBM equation, in the $\mathbb{L}^2$-, $\mathbb{H}^1$, and $\mathbb{L}^\infty$-norm (left, middle, and right, respectively).

where δ is the true rate of convergence in probability, and h_{max}, h_{min} are the greatest and smallest time step sizes considered in the experiment. This factor appears in the converse of Proposition 2.7.1, illustrated in the left image of Figure 2.8. The similarity in shape indicates that the assumptions for Proposition 2.7.1, while harsh, are partially motivated.

To lessen the harsh assumption made in Proposition 2.7.1, one can instead observe a similar integral. For some interval $S \subset (0, \hat{h}]$, define

$$C(S, \varepsilon, \delta) = \inf \left\{ C \in \mathbb{R}^+ : \forall h \in S \quad \mathbb{P}\left(e(T, N, \mathcal{N}, \omega) \geqslant C(\varepsilon) h^\delta \right) < \varepsilon \right\}.$$

Then define the integral

$$k(S, \delta, p) = \int_0^1 \left\| \log(C(S, \varepsilon, \delta) h^\delta) - \log(F_h^{-1}(\varepsilon)) \right\|_{L^p(\hat{S})} \mathrm{d}\varepsilon$$

where $h \in \hat{S} = \{\log(s)\}_{s \in S}$.

Take some initial $\tilde{h} < \hat{h}$ and define the sequence

$$\begin{cases} S_n &= S_{n-1} \cup (\tilde{h}/2^n, \tilde{h}/2^{n-1}] \\ S_0 &= (\tilde{h}/2, \tilde{h}] \end{cases}.$$

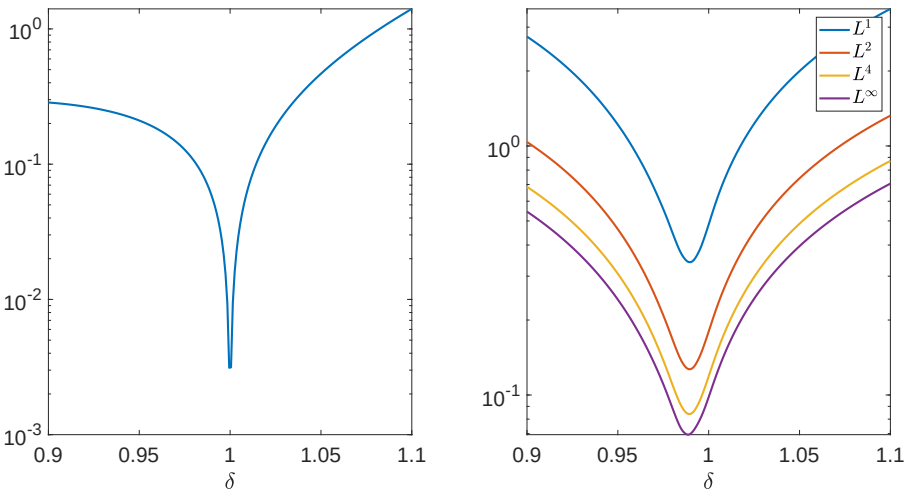

Figure 2.8: Left image: $|h_{max}^{-a} - h_{min}^{-a}|$ for $a = \hat{\delta} - \delta$ with $\delta = 1$. Right image: Using the k-estimation method, estimating $k(S, \delta, p)$ for $p = 1, 2, 4, \infty$, using the SE for the SBBM.

Then we conjecture that for all $p \geqslant 1$,

$$\lim_{n \to \infty} \frac{k(S_n, \delta, p)}{k(S_n, \hat{\delta}, p)} = 0$$

for $\hat{\delta} \neq \delta$ if and only if the numerical scheme converges with order δ. We call this method of numerically demonstrating the order of convergence in probability the k-estimation method. As an example, in the right image of Figure 2.8, we can see $k(S, \delta, p)$ estimated for $p = 1, 2, 4, \infty$ using the SE for the SBBM and $\mathbb{H}^1$-norm.

2.7.3 Almost sure convergence

As with the numerical illustration of the order of convergence in probability, few attempt to numerically illustrate the almost sure order of convergence in the literature. Some attempts to inspect the convergence rate of single samples exist, e.g., [23], while a multi-sample approach is rarer [11].

To estimate the rate of almost sure convergence, we again estimate the translation coefficient. Only this time, we take a fixed sample ω, yielding

$$K_\delta(T, \mathcal{N}, \omega) = \arg\inf_h \{C \in \mathbb{R}^+ : Ch^\delta \geqslant e(T, N, \mathcal{N}, \omega)\},$$

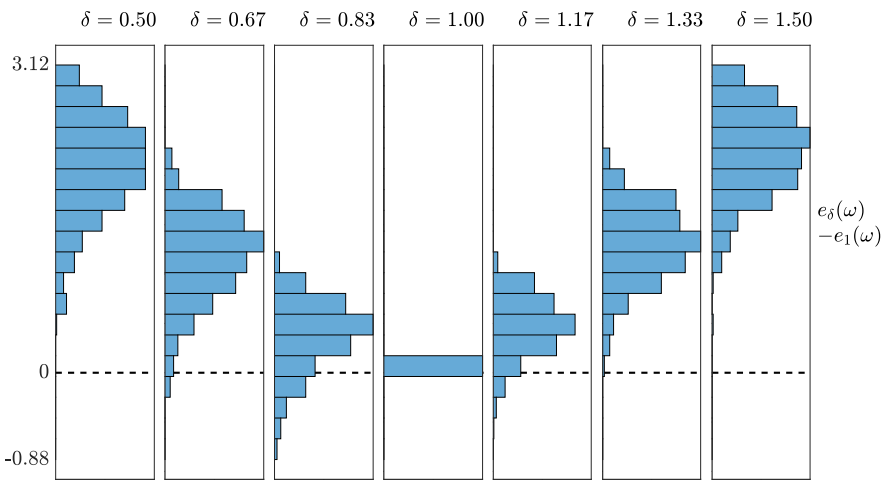

Figure 2.9: Using the $e_\delta(\omega)$-estimation method, an illustration of the almost sure convergence rate of the SE for the SBBM equation, in the $\mathbb{H}^1$-norm.

for all considered time-step sizes h. For a sufficiently large span of h, we would then expect that the distance

$$e_\delta(\omega) = e_\delta(\omega, T, \mathcal{N}) = \sup_h |K_\delta(T, \mathcal{N}, \omega)h^\delta - e(T, N, \mathcal{N}, \omega)|$$

would be minimized for the correct order of convergence δ. A number of histograms of $e_\delta(\omega, 1, \mathbb{H}^1) - e_1(\omega, 1, \mathbb{H}^1)$ for SE for the SBBM can be seen in Figure 2.9. We can observe that with the exception of a few samples, $e_\delta(\omega, 1, \mathbb{H}^1)$ is minimized for $\delta = 1$ and that the rate of convergence is close to $\delta = 1$ for the rest. These results indicate that the SE converges almost surely with an order close to 1 with respect to the $\mathbb{H}^1$-norm.

This method of illustrating the almost surely convergence rate is sensitive to the range of h considered, given that each sample may fluctuate in precision wildly. A greater span of h will ensure that the distributions of errors, as seen in Figure 2.1, overlap less, leading to better estimations of $e_\delta(\omega)$.

3

The Stochastic Models Studied in the Thesis

3.1 Common notation

Let $(\Omega, \mathcal{F}, \mathbb{P})$ be a probability space. On this probability space, define a real-valued standard Brownian motion $W : \mathbb{R}^+ \to \mathbb{R}$. We endow the probability space with the complete filtration $\{\mathcal{F}_t\}_{t \geqslant 0}$ generated by W. The SPDEs are interpreted in the Stratonovich sense, see Section 2 for the definition of the Stratonovich product, and the initial value is denoted X_0.

We use I to denote the identity operator. For $X : [0, T] \times \mathbb{R} \to \mathbb{C}$ we denote the first and second order spatial derivatives along the second variable x as

$$X_x = \partial_x X = \frac{\partial X}{\partial x},$$

$$X_{xx} = \partial_x^2 X = \frac{\partial^2 X}{\partial x^2}.$$

Similarly, for $X : [0, T] \times \mathbb{R}^n \to \mathbb{C}$ we denote the Laplacian as

$$\Delta X = \sum_{j=1}^{n} \partial_{x_j}^2 X.$$

Lastly, each equation below contains power law nonlinearities of the form $|X|^\sigma X$ for some $\sigma > 0$. In the case where X maps onto $\mathbb{C}^2$, $|X|^2$ is interpreted as the coupling $|X|^2 = |X^1|^2 + |X^2|^2$.

3.2 The Stochastic Nonlinear Schrödinger Equation with White Noise Dispersion

3.2.1 Area of application

As described in the introduction, the nonlinear Schrödinger equation (NLSE) can be applied to optical signals [97]. More generally, it is suitable to describe wave propagation in nonlinear media [97], including surface waves on deep water [78], or even Bose–Einstein condensates [97, 38] (the NLSE is then known as the Gross–Pitaevskii equation).

From the perspective of light propagation, the stochastic nonlinear Schrödinger equation with white noise dispersion (SNLSE) models the dispersion of the optical signal as it travels through the fiber [70, 14, 29]. See Section 4.3 for more details on the derivation of the NLSE and the SNLSE.

3.2.2 The definition and an evolution illustration

In paper [13], we perform a numerical study of the **stochastic nonlinear Schrödinger equation with white noise dispersion** (SNLSE)

$$i\mathrm{d}X + \alpha\Delta X \circ \mathrm{d}W + \beta|X|^{2\sigma}X\,\mathrm{d}t = 0$$

where i is the imaginary unit, $X : \mathbb{R}^+ \times \mathbb{R}^n \times \Omega \to \mathbb{C}$ is unknown, $\alpha, \beta \in \mathbb{R}$ are known, and $\sigma \in \mathbb{R}^+$ is the nonlinearity parameter.

An illustration of how the time evolution of a numerical realization to the SNLSE is presented in Figure 3.1. The evolution starts with a Gaussian initial value, $X_0(x) = \exp(-3x^2)$, and it is clearly visible how the intensity disperses and contracts over time.

3.2.3 Conjecture on the critical exponent

The deterministic NLSE

$$i\mathrm{d}X + \alpha\Delta X\,\mathrm{d}t + \beta|X|^{2\sigma}X\,\mathrm{d}t = 0$$

is globally well posed in $L^2(\mathbb{R}^n)$ [29, 45, 57, 98] for $\sigma < 2/n$. The quantity $\sigma = 2/n$ is referred to as the critical exponent. The question of existence and well-posedness of the SNLSE is not straightforward. Existence of local solutions for the SNLSE has been shown in [14] for the values

$$\frac{2}{n} \leqslant \sigma < \frac{2}{n-2}.$$

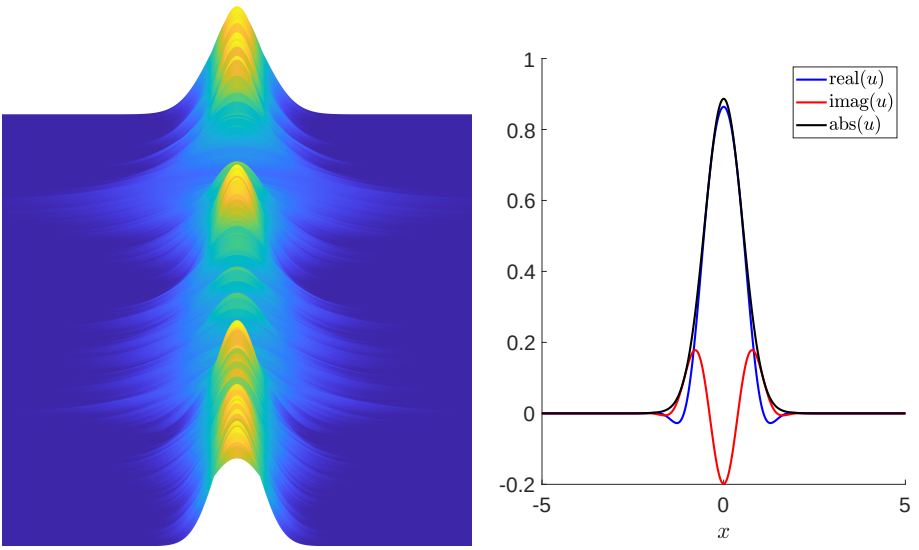

Figure 3.1: Using a Gaussian initial value, $X(0) = \exp(-3x^2)$, the evolution of the intensity, $|X|^2$, of an SNLSE sample over $t \in [0, 1/4]$ (left) and the final outcome at $t = 1/4$ (right).

The SPDE has global solutions for

$$\sigma < \frac{2}{n},$$

see [14, Theorem 2.1], and for $n = 1$, $\sigma = 2$ [29, Theorem 2.1]. It is then conjectured in [7] that the critical exponent in the SNLSE is twice that of the NLSE, meaning $\sigma = 4/n$ instead of $\sigma = 2/n$.

This conjecture has been extensively tested numerically throughout the literature and this thesis.

3.3 The Stochastic Manakov Equation

3.3.1 Area of application

While the NLSE appears in a number of applications, the MPMDE (see Section 1.1.2) is more specific, focusing mainly on light propagation though optical fibers. To be specific, the MPMDE and SME decompose the light wave into two modes of polarization and consider how these polarizations

affect each other. See Section 4.2 for more details. It is recommended to approach simulating light propagation using different models depending on the scale [73]. The MPMDE is recommended at the longest scale, corresponding to tens to thousands of kilometers.

3.3.2 The definition and an evolution illustration

We consider the **stochastic (nonlinear) Manakov system** (SME) [43]

$$i\mathrm{d}X + \partial_x^2 X\,\mathrm{d}t + |X|^{2\sigma} X\,\mathrm{d}t + i\sqrt{\gamma}\sum_{k=1}^{3}\sigma_k \partial_x X \circ \mathrm{d}W_k = 0, \tag{3.1}$$

where W_1, W_2, W_3 are independent standard Brownian motions, W is the three-dimensional standard Brownian motion

$$W(t) := (W_1(t), W_2(t), W_3(t)),$$

$X : \mathbb{R}^+ \times \mathbb{R} \times \Omega \to \mathbb{C}^2$ is unknown with the components $X = (X^1, X^2)$, $\gamma \geqslant 0$ measures the intensity of the noise, the nonlinear coupling is denoted by $|X|^2 = |X^1|^2 + |X^2|^2$, $\sigma \in \mathbb{R}^+$ is the nonlinearity parameter and σ_1, σ_2 and σ_3 are the classical Pauli matrices (see Section 4.4) defined by

$$\sigma_1 = \begin{pmatrix} 0 & 1 \\ 1 & 0 \end{pmatrix}, \qquad \sigma_2 = \begin{pmatrix} 0 & -i \\ i & 0 \end{pmatrix}, \quad \text{and} \quad \sigma_3 = \begin{pmatrix} 1 & 0 \\ 0 & -1 \end{pmatrix}.$$

An illustration of how the time evolution of the numerical realization to the SME is presented in Figure 3.2. The evolution starts with a Gaussian initial value for each component, with maximum height 1 and different translations. It is clear that the dispersion is not as straightforward as for the SNLSE.

3.4 The Stochastic Generalized Benjamin–Bona–Mahony Equation

3.4.1 Area of application

The KdV and BBM equations have a lot of common applications, which is natural given that BBM was proposed as an alternative to the KdV equation. These models describe long-wave propagation in nonlinear media, allowing many physical interpretations. Some examples are waves in water [61, 40, 81, 8], crystals [44], or plasma [40, 104, 18].

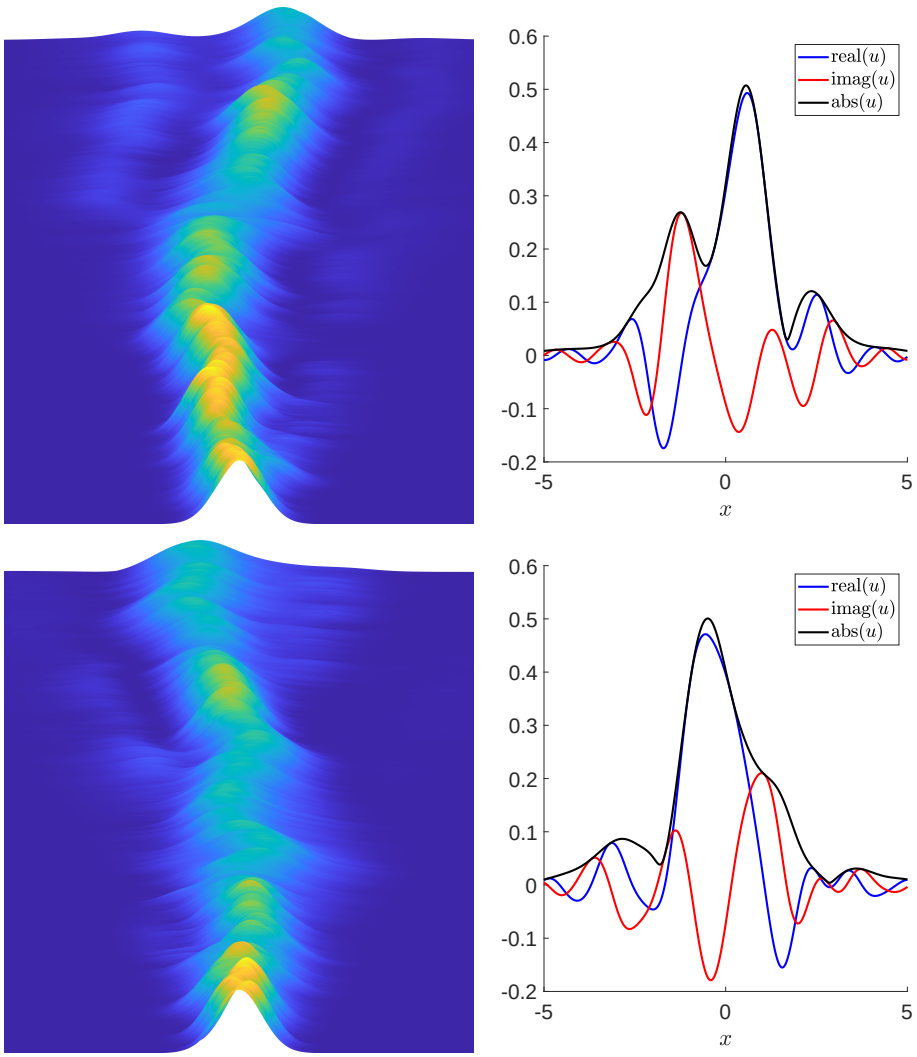

Figure 3.2: Using a Gaussian initial value, $X^1(0) = X^2(0) = \exp(-3x^2)/\sqrt{2}$, the evolution of the intensity, $|X^i|^2$, $i = 1, 2$, of the components of the SME (first component top, second component bottom) over $t \in [0, 1/4]$ (left) and the final outcome at $t = 1/4$ (right).

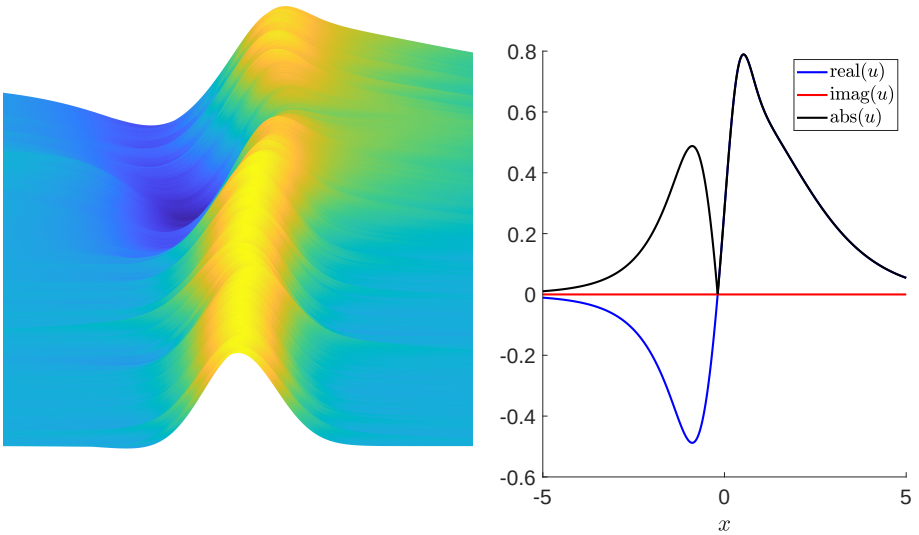

Figure 3.3: Using a Gaussian initial value, $X(0) = \exp(-3x^2)$, the evolution of the SBBM over $t \in [0, 10]$ (left) and the final outcome at $t = 10$ (right).

From the perspective of water wave propagation, it becomes clear that stochasticity is present. Examples include the water surface interacting with the air through wind or the water interacting with uneven bottom geography [21].

3.4.2 The definition and an evolution illustration

The **stochastic generalized Benjamin–Bona–Mahony equation with white noise dispersion** (SBBM) [21]:

$$\left(I - \partial_x^2\right) \mathrm{d}X + \left(\alpha\partial_x^2 - \beta I\right) X \mathrm{d}t + \frac{\partial_x}{\sigma + 1} X^{\sigma+1} \mathrm{d}t + \partial_x X \circ \mathrm{d}W = 0, \quad (3.2)$$

where $X : \mathbb{R}^+ \times \mathbb{R} \times \Omega \to \mathbb{R}$ is unknown, and $\alpha, \beta \in \mathbb{R}$, $\sigma \in \mathbb{R}^+$ are known.

An illustration of how the time evolution of a numerical realization to the SBBM (observe: not the intensity, as with the SNLSE and the SME) is presented in Figure 3.3. The evolution starts with a Gaussian initial value, with maximum height 1. Although the influence of the white noise on the wavefront is not very noticeable at the scale of the experiment, an effect can be observed in the spreading and retracting of the wavefront.

4

The Derivations of the Light-Propagation Models

In this section we present and derive the Nonlinear Schrödinger Equation (NLSE, see e. g. [36, 16]), the Manakov Equation (MPMDE, see e. g. [68]), and to a lesser extent the Stochastic Non-Linear Schrödinger Equation with white noise dispersion (SNLSE, see e. g. [7]), and the Stochastic Manakov Equation (SME, see e. g. [43]). More references can be seen in each of the following subsections.

These (stochastic) partial differential equations can be derived using the fields

$$\vec{E}, \vec{H}, \vec{D}, \vec{B} : \mathbb{R}^+ \times \mathbb{R}^3 \to \mathbb{C}^3,$$

which are called the electric, magnetic, electric induction (or displacement), and magnetic induction fields, respectively. These fields are related through the Maxwell–Faraday equation (MF), the Maxwell–Ampère equation (MA), Gauss's law (G), and Gauss's law for magnetism (GL):

$$\begin{aligned} \text{(MF)} \quad & \nabla \times \vec{E} = -\frac{\partial \vec{B}}{\partial t}, & \text{(MA)} \quad & \nabla \times \vec{H} = \vec{J} + \frac{\partial \vec{D}}{\partial t}, \\ \text{(G)} \quad & \nabla \cdot \vec{D} = \rho, & \text{(GL)} \quad & \nabla \cdot \vec{B} = 0, \end{aligned}$$

where $\vec{J} = \vec{J}(x, y, z, t)$ is the conductivity field of the material, $\rho = \rho(x, y, z, t)$ is the (constant) free charge density, $\nabla\times$ is the curl, and $\nabla\cdot$ is the divergence. Collectively, these equations are referred to as Maxwell's equations [2]. Aside from the above system of equations, we need to introduce the electric polarization field $\vec{P} = \vec{P}\left(\vec{E}\right)$ and two constitutive relations:

$$\vec{B} = \mu_0 \vec{H} \qquad \vec{D} = \varepsilon_0 \vec{E} + \vec{P}, \tag{4.1}$$

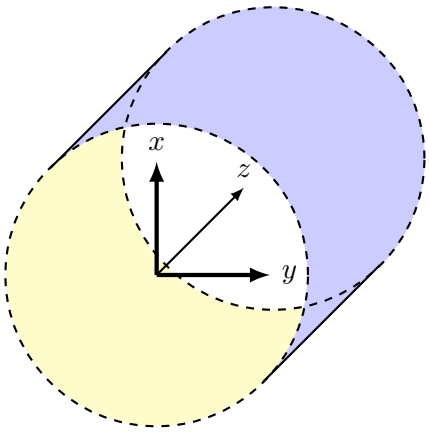

Figure 4.1: Fiber cross section.

where μ_0 and ε_0 are the magnetic permeability and vacuum permitivity, respectively. These constants are related by $\varepsilon_0\mu_0 = c^{-2}$, where c is the speed of light in a vacuum.

The derivations of the NSLE, SNLSE, MPMDE, and SME, below, are based on the perspective of light propagating through a cylindrical optical fiber, see Figure 4.1, made of an isotropic medium such as glass. In each subsection, we will go more into depth about the assumptions made, as well as their interpretations and implications.

The NLSE, and similar equations, can be derived through modeling other phenomena as well. We will not concern ourselves with those more than necessary, but some examples include water waves over deep water [82, 56], gravity waves [37], or Bose–Einstein condensates [32, 28]. Research around Bose–Einstein condensates is a very active area at the moment, and the NLSE appears in the shape of the Gross–Pitaevskii equation, derived independently by Eugene P. Gross and Lev Petrovich Pitaevskii as far back as 1961 [47, 83].

4.1 The deterministic nonlinear Schrödinger equation

For more on the NLSE , e. g. the properties, or further details on the derivation, we refer the reader to e. g. [2, 16, 36, 97, 105].

To simplify our derivation, we begin by introducing the following assump-

tions regarding the medium which the light propagates through:

Assumption 1: The medium is a cylindrical optical fiber, see Figure 4.1.

Assumption 2-4: The material of the fiber has the following properties:

- It is isotropic and homogeneous. This means that the material has identical properties independently of direction (isotropic) and position (homogeneous).
- It has zero free charge density, $\rho = 0$, as seen in Equation (G). This would otherwise influence the displacement $\vec{D}$ and magnetic $\vec{H}$ fields, through Equation (4.1).
- It has zero conductivity, $\vec{J} = 0$. This prevents the electric field from inducing an electric current through the material, via Equation (MA).

If we were to have a cylindrical fiber of pure silica, i. e. Silicon Dioxide or SiO_2, with no charge, we would fulfill these requirements since silica has a near-zero conductivity coefficient between 10^{-23} to 10^{-27} (which is considered to be lossless in practice). Further assumptions are made along the derivation of the NLSE below. We also want to stress that there is a valid criticism to be made, in terms of realistic assumptions, as mentioned in [73].

Disregarding this criticism, we deduce from Maxwell's equations and the first constitutive relation in (4.1) that

$$\nabla \times (\nabla \times \vec{E}) = \nabla \times \left(-\frac{\partial \vec{B}}{\partial t} \right) = -\frac{\partial}{\partial t} \left(\nabla \times \mu_0 \vec{H} \right) = -\mu_0 \frac{\partial}{\partial t} \frac{\partial}{\partial t} \vec{D},$$

which is equivalent to

$$\nabla \times (\nabla \times \vec{E}) + \frac{1}{c^2 \varepsilon_0} \frac{\partial^2}{\partial t^2} \vec{D} = 0.$$

Applying the vector identity

$$\nabla \times (\nabla \times \vec{E}) = -\Delta \vec{E} + \nabla (\nabla \cdot \vec{E})$$

yields

$$\nabla (\nabla \cdot \vec{E}) - \Delta \vec{E} + \frac{1}{c^2 \varepsilon_0} \frac{\partial^2}{\partial t^2} \vec{D} = 0.$$

By using that the divergence of $\vec{P}$ is usually negligibly small, we can simplify the equation above. If we combine Gauss's law (G), the second constitutive

relation in (4.1), and the assumption that the free charge density ρ is 0, we have

$$0 = \rho = \nabla \cdot \vec{D} = \nabla \cdot (\varepsilon_0 \vec{E} + \vec{P}) \approx \varepsilon_0 \nabla \cdot \vec{E},$$

which gives us

$$\Delta \vec{E} - \frac{1}{c^2 \varepsilon_0} \frac{\partial^2}{\partial t^2} \vec{D} = 0. \tag{4.2}$$

The above equation is known as Maxwell's wave equation [2].

To further simplify the derivation, we assume that the electrical field is of the form

$$\vec{E}(x, y, z, t) = e^{-i\omega_0 t} \vec{\mathcal{E}}(x, y, z) + e^{i\omega_0 t} \overline{\vec{\mathcal{E}}}(x, y, z), \tag{4.3}$$

where ω_0 is the frequency of the electrical field oscillations. We also assume that $\vec{E}$ is linearly polarized. Linear polarization gives that the fields $\vec{D}$, $\vec{E}$, and $\vec{P}$ are of the form $\vec{D} = (D, 0, 0)$, $\vec{E} = (E, 0, 0)$, and $\vec{P} = (P, 0, 0)$.

When an electric field $\vec{E}$ is applied to a material, the refraction index, see definition further down, changes in response. For silica, despite being negligible in short distances, this effect becomes relevant when we cover long distances seen in e. g. transcontinental fiber optics. We, therefore, expand P in a Taylor series, soon approximating its nonlinear influence:

$$P(E) = \varepsilon_0 \sum_{k=0}^{\infty} \chi^{(k)}(\omega_0) E^k.$$

Due to a phenomenon known as "inversion symmetry" [2], which holds for isotropic materials, the even-order terms in the above sum are zero,

$$\chi^{(2j)} = 0, \quad j = 0, 1, \ldots.$$

When we truncate the above sum by the leading nonlinear term we hence get

$$P(E) \approx \varepsilon_0 \left(\chi^{(1)}(\omega_0) E + \chi^{(3)}(\omega_0) E^3 \right). \tag{4.4}$$

By only considering the frequency ω_0 and inserting Equation (4.3) into Equation (4.4), we get the approximation

$$\begin{aligned} P(E) &\approx \varepsilon_0 \left(\chi^{(1)}(\omega_0) E + \chi^{(3)}(\omega_0) E^3 \right) \\ &= \varepsilon_0 \left(\chi^{(1)}(\omega_0) E + \chi^{(3)}(\omega_0) \left(\sum_{k=0}^{3} \binom{3}{k} e^{-i(3-2k)\omega_0 t} \mathcal{E}^{3-k} \bar{\mathcal{E}}^k \right) \right) \\ &\approx \varepsilon_0 E \left(\chi^{(1)}(\omega_0) + 3\chi^{(3)}(\omega_0) |\mathcal{E}|^2 \right). \end{aligned}$$

Inserting the above into the second constituent relation in (4.1) yields us that

$$D \approx \varepsilon_0 E \left(1 + \chi^{(1)}(\omega_0) + 3\chi^{(3)}(\omega_0)|\mathcal{E}|^2\right) =: \varepsilon_0 E\, n^2(\omega_0, |\mathcal{E}|^2), \tag{4.5}$$

where n^2 is known as the refraction index of the material. This dependence on $|\mathcal{E}|^2$ is known as the Kerr, or the quadratic electro-optic, effect. Inserting Equation (4.5) into Equation (4.2) yields two conjugate equations, that reduce to

$$\Delta\mathcal{E}(x,y,z) + \frac{n^2\omega_0^2}{c^2}\mathcal{E}(x,y,z) = 0, \tag{4.6}$$

which we know as the scalar nonlinear Helmholtz equation [2]. Defining

$$k_0^2 = \frac{\omega_0^2(1 + \chi^{(1)}(\omega_0))}{c^2}, \tag{4.7}$$

substituting

$$\mathcal{E}(x,y,z) = e^{ik_0 z}\psi(x,y,z)$$

in Equation (4.6), and applying the paraxial approximation $\psi_{zz} \ll k_0\psi_z$ yields

$$\begin{aligned}\Delta\mathcal{E} + \frac{n^2\omega_0^2}{c^2}\mathcal{E} &= e^{ik_0 z}\left(-k_0^2\psi + 2ik_0\psi_z + \psi_{zz} + \psi_{xx} + \psi_{yy} + \frac{n^2\omega_0^2}{c^2}\psi\right)\\ &\approx e^{ik_0 z}\left(2ik_0\psi_z + \Delta_\perp\psi + \frac{3\chi^{(3)}(\omega_0)\omega_0^2}{c^2}|\psi|^2\psi\right) = 0,\end{aligned}$$

where $\Delta_\perp = \frac{\partial^2}{\partial x^2} + \frac{\partial^2}{\partial y^2}$. This gives us the NLSE

$$2ik_0\psi_z + \Delta_\perp\psi + \frac{3\chi^{(3)}(\omega_0)\omega_0^2}{c^2}|\psi|^2\psi = 0, \tag{4.8}$$

where $\psi : \mathbb{R}^3 \to \mathbb{C}$ and z acts as the time (also known as the retarded time).

4.2 The deterministic Manakov equation

Continuing with the interpretation of light propagating through a fiber, we now note that light waves can be expressed in terms of polarized components, see Figure 4.2, and we, therefore, can build the MPMDE by coupling two NLSEs. For the more dedicated reader, we refer to, e.g., [2, Ch. 6] or

the articles by Menyuk et al. [71, 72, 74, 75, 73]. One of the shortest routes to arrive at the MPMDE would be to follow [68]. Note that this derivation relies on ψ having a slightly different domain than in the previous, $\psi : \mathbb{R}^+ \times \mathbb{R}^3 \to \mathbb{C}$. We start by recalling that the factor $|\psi|^2$ in (4.8) represents the total intensity of the light. With this we represent the electric field by two orthogonal polarizations: $\psi = E^1\vec{v}_1 + E^2\vec{v}_2$, where $\vec{v}_1, \vec{v}_2 : \mathbb{R}^+ \times \mathbb{R}^3 \to \mathbb{C}$. If we slightly rewrite the NLSE, representing the electrical field as it traverses the length of the fiber to

$$i\psi_z + \Delta_\perp \psi + |\psi|^2\psi = 0,$$

we immediately get the coupled equations:

$$\begin{aligned} iE^1_z + \Delta_\perp E^1 + (|E^1|^2 + |E^2|^2)E^1 = 0 \\ iE^2_z + \Delta_\perp E^2 + (|E^1|^2 + |E^2|^2)E^2 = 0. \end{aligned}$$

By defining $X = (X_1, X_2) = (E^1, E^2)$, redefining $t = z$, we get the MPMDE:

$$iX_t + \Delta_\perp X + |X|^2 X = 0, \tag{4.9}$$

where $X = X(t, x, y) = (X_1, X_2)$ is the unknown vector-valued function with values in $\mathbb{C}^2$, and $|X|^2 = |X_1|^2 + |X_2|^2$ is the nonlinear coupling.

4.3 The stochastic nonlinear Schrödinger equation

For additional articles on the SNLSE, we refer the reader to [70, 14, 29, 7, 22, 25, 95]. We follow the derivation presented in [70, 14]. Starting with the equation

$$\begin{aligned} i\mathrm{d}v + \varepsilon m(t)\Delta v\mathrm{d}t + \varepsilon^2|v|^{2\sigma}v\mathrm{d}t = 0 \\ v(0) = v_0, \end{aligned}$$

where m is a stationary stochastic process with mean zero, $\varepsilon > 0$, v_0 is the initial value, and $\sigma > 0$. We motivate why the above equation is possible by imagining that we construct an optical fiber by appending lengths of fibers to each other, with coefficients $\chi^{(1)}$ and $\chi^{(3)}$, see Equations (4.7) and (4.8), such that the desired outcome is achieved. Rescaling the time variable according to

$$u(t, x) = v\left(\frac{t}{\varepsilon}, x\right)$$

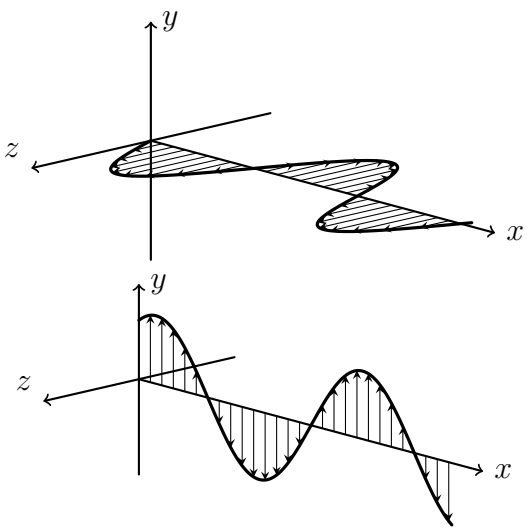

Figure 4.2: Two orthogonal light waves travelling along the x-axis, courtesy of [76].

yields the equation

$$i\mathrm{d}u + \frac{1}{\varepsilon}m\left(\frac{1}{\varepsilon^2}\right)\Delta u\,\mathrm{d}t + |u|^{2\sigma}u\,\mathrm{d}t = 0$$
$$u(0) = u_0.$$

Letting $\varepsilon \to 0$, see [14, 70, 79], classical ergodic assumptions yield the SNLSE

$$i\mathrm{d}u + \sigma_0\Delta u \circ \mathrm{d}\beta + |u|^{2\sigma}u\,\mathrm{d}t = 0$$
$$u(0) = u_0, \tag{4.10}$$

where β is a standard Brownian motion with variance σ_0^2 calculated using the covariance function of m, r_m, via

$$\sigma_0^2 = 2\int_0^\infty \mathbb{E}\left[m(0)m(t)\right]dt = 2\int_0^\infty r_m(t)\,dt.$$

We want to stress that Equation (4.10) is understood in the Stratonovich sense, using the $\circ$ symbol for the Stratonovich product.

4.4 Polarized light and the Poincaré sphere

Polarization is a fundamental characteristic of light and for more materials on the following topics the reader is referred to e.g. [24, 2, 39]. This section will only briefly present some concepts related to polarization, namely: The Poincaré sphere, the Stokes parameters (or Stokes vector), birefringence, and polarization-mode dispersion.

The Poincaré sphere, see Figure 4.3, originates as far back as 1892 [85, 84, 87], and can be used to uniquely represent the polarization states. Any point on the Poincaré sphere can be expressed as $P = (S_1, S_2, S_3)$, where S_i, $i = 1, 2, 3$, are the Cartesian coordinates, also known as the Stokes parameters. If we complete the classical Pauli matrices $\sigma_i, i = 1, 2, 3$, with the identity matrix to complete the basis for the real vector space of 2×2 Hermitian matrices, we get

$$I = \sigma_0 = \begin{pmatrix} 1 & 0 \\ 0 & 1 \end{pmatrix}, \qquad \sigma_1 = \begin{pmatrix} 0 & 1 \\ 1 & 0 \end{pmatrix},$$
$$\sigma_2 = \begin{pmatrix} 0 & -i \\ i & 0 \end{pmatrix}, \quad \text{and} \quad \sigma_3 = \begin{pmatrix} 1 & 0 \\ 0 & -1 \end{pmatrix},$$

and we can express the Stokes vector of a polarization state $X = (u, v)$. Following the notation of [34], we get

$$S = \begin{pmatrix} S_0 \\ S_1 \\ S_2 \\ S_3 \end{pmatrix} = \begin{pmatrix} X^\dagger \sigma_0 X \\ X^\dagger \sigma_1 X \\ X^\dagger \sigma_2 X \\ X^\dagger \sigma_3 X \end{pmatrix} = \begin{pmatrix} |u|^2 + |v|^2 \\ |u|^2 - |v|^2 \\ \bar{u}v + \bar{v}u \\ -i(\bar{u}v - \bar{v}u) \end{pmatrix} \in \mathbb{R}^+ \times \mathbb{R}^3,$$

where $X^\dagger$ is the complex conjugate transpose of X, and S_0 is the radius of the sphere, fulfilling $S_0^2 = S_1^2 + S_2^2 + S_3^2$.

In Section 4.1 we stressed that the assumptions made for the derivation of the NLSE may not be realistic. For example, they can be violated by introducing stress, twisting, turning, or simply misshaped cores. This affects the refractive index, leading to the two orthogonal polarizations, as introduced in Section 4.2, behaving differently. This phenomenon is known as birefringence, see e.g. [2]. For light propagation over long distances, the phenomenon known as polarization-mode dispersion (or PMD) becomes very important, as it causes different delays to different polarizations. This has been widely studied, see e.g. the references in [39] for a number of articles on the subject.

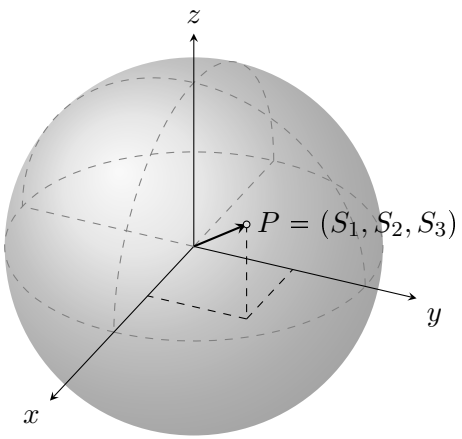

Figure 4.3: The Poincaré sphere, courtesy of [9].

4.5 The stochastic Manakov equation

The SME that we consider is known as the Manakov PMD equation. The original equation was introduced in [75] which, due to the different scales present in the modelling, contained a parameter ε. The limit equation, when $\varepsilon \to 0$, was investigated for the linear case in [69, 41], and the nonlinear case in [15, 42]

We stress that the exact derivation of the nonlinear SME is lengthy and difficult. For the interested reader we refer to [15] and limit the following text to only contain some of the key points to the derivation. We denote the group velocity dispersion parameter and birefringence strength with d_0 and b respectively. Moreover, $\nu_\varepsilon(t) = \nu(t/\varepsilon^2)$ is a stochastic process almost surely on the unit sphere, and

$$\begin{aligned}\sigma(u(t)) &= \begin{bmatrix} |u_1(t)|^2 - |u_2(t)|^2 & 2\bar{u_1}\bar{u_2} \\ 2u_1u_2 & |u_2(t)|^2 - |u_1(t)|^2 \end{bmatrix} \\ &= \begin{bmatrix} m_3 & m_1 - im_2 \\ m_1 + im_2 & -m_3 \end{bmatrix} = \sigma_1 m_1(t) + \sigma_2 m_2(t) + \sigma_3 m_3(t),\end{aligned}$$

where m_i, $i = 1, 2, 3$, are some real-valued processes. Finally, $F_{\nu_\varepsilon(t)}$ is a nonlinearity with a coupling similar to the coupling in the MPMDE, but affected by ν_ε (and in extension by the processes m_i, $i = 1, 2, 3$). With all these components we consider Equation (1.11) in [15]

$$i\frac{\partial X_\varepsilon(t)}{\partial t} + \frac{d_0}{2}\frac{\partial^2 X_\varepsilon(t)}{\partial x^2} + \frac{ib'}{\varepsilon}\sigma(\nu_\varepsilon(t))\frac{\partial X_\varepsilon(t)}{\partial x} + F_{\nu_\varepsilon(t)}(X_\varepsilon(t)) = 0,$$

and let $\varepsilon \to 0$. We then get, [15, Theorem 1.3], the SME

$$i\mathrm{d}X + \frac{d_0}{2}\partial_x^2 X\,\mathrm{d}t + i\sqrt{\gamma}\sum_{k=1}^{3}\sigma_k\partial_x X \circ \mathrm{d}W_k + \frac{8}{9}|X|^2 X\,\mathrm{d}t = 0, \tag{4.11}$$

where $W = (W_1, W_2, W_3)$ is a $3d$ Brownian motion, $\gamma \geqslant 0$ measures the intensity of the noise, and $|X|^2 = |X_1|^2 + |X_2|^2$ is the nonlinear coupling. As a consequence of the Brownian motion, the polarization state of the solution to the SME will change randomly over time, maintaining the Stokes vector on the Poincaré sphere.

5 Future Work

As can be seen, the exponential and splitting integrators have emerged as promising approaches. However, within the context of this thesis, several questions remain unanswered. In the following list, when we refer to convergence rates we specifically refer to strong, in probability, and almost sure convergence rates for appropriate norms. The potential avenues for future research include, but are not limited to, the following.

Regarding the exponential and splitting integrators for the stochastic Benjamin–Bona–Mahony equation (3.2), there are a number of potential questions. The following points are indicated by numerical experiments in [10]. It would be interesting to:

- Prove that the convergence rates of the explicit exponential integrator has order 1.
- Prove that the convergence rates of the symmetric exponential, Lie–Trotter splitting, and Strang splitting integrators have order 1 in the nonlinear case ($\sigma > 0$) of the stochastic Benjamin–Bona–Mahony equation.
- Prove that the convergence rates of the symmetric exponential integrator has order 2 for the (deterministic) Benjamin–Bona–Mahony equation.
- Prove that the convergence rates of the symmetric exponential, Lie–Trotter splitting, and Strang splitting integrators have order 2 for the linear case ($\sigma = 0$) of the stochastic Benjamin–Bona–Mahony equation.

- Prove that the symmetric exponential integrator for the stochastic Benjamin–Bona–Mahony equation preserves the H^1-norm when $\alpha = \beta = 0$.

Similarly, it would be interesting to prove the convergence rates for the symmetric exponential integrator for the stochastic Manakov equation (3.1), see [11, 12] for numerical experiments.

A lot of work has gone into exploring the critical exponents, see Section 3.2.3 and [13] for Equation (3.1) and [11] for Equation (3.1). This work can be expanded upon, both theoretically and numerically. Especially interesting would be working towards observing Equation (3.1) defined on the real line, since some work has been observed for Equation (3.1) defined on the torus [95]. Naturally, in the case of a numerical investigation, it would be wise to use as many time-saving methods as is feasible, see [13] for a few.

There's still work to be done improving upon the illustration methods for the convergence in probability, see Section 2.7.2. This can either be done by investigating the $I(\delta)$-estimation method, e.g. by improving Proposition 2.7.1 or by observing its converse. It would also be interesting to formalize and prove the conjecture regarding the k-estimation method, which states: For all $p \geqslant 1$

$$\lim_{n\to\infty} \frac{k(S_n, \delta, p)}{k(S_n, \hat{\delta}, p)} = 0$$

for $\hat{\delta} \neq \delta$ if and only if the numerical scheme converges with order δ.

Similarly, work can be done on the numerical illustration method of the almost sure convergence rate. See Section 2.7.3. Given that the $e_\delta(\omega)$-estimation method, shown in Figure 2.9, is a first attempt, it can likely be improved both in presentation and in approach.

Lastly, splitting and exponential integrators can (naturally) be adapted to more SPDEs than considered within this thesis. This can be done in a number of ways, but three stand out. The first would be to introducing these integrators to an SPDE where they have not yet been implemented. The second way would be to introduce noise to a PDE currently lacking the corresponding SPDE, and then introducing these integrators. This could potentially draw from already existing implementations and theory, see e.g. the quasilinear Maxwell's equations [30] or the nonlinear Helmholtz equation [92]. The third way would be to consider different types of stochastic processes, such as Poisson [60], Lévy [58], or Q-Wiener processes [27].

6

Summaries and Contributions of the Articles

As a convention: Whenever convergences are mentioned in this section, we are talking about convergences in time, as mentioned in Section 2.6.

For code related to these articles, see `https://bitbucket.org/BergCode/spde_simulation/src/master/`. The repository includes several numerical experiments for each SPDE model, implemented in Matlab.

6.1 Numerical study of nonlinear Schrödinger equations with white noise dispersion [13]

We perform a numerical analysis of the stochastic nonlinear Schrödinger equation with white noise dispersion (SNLSE). By carrying out a number of numerical experiments we illustrate quantitative and qualitative behaviors of solutions to this SPDE. In particular, we perform a large number of numerical experiments, in 1 and 2 dimensions, investigating the conjecture posed in [14, 7]. Furthermore, we collect a number of numerical integrators and thoroughly compare their performance. For instance, these experiments illustrate the types of convergence mentioned in Section 2.6, the preservation of the L^2-norm, and the computational time of the integrators.

Contributions: I designed and executed most of the numerical experiments. Based on a first draft, I wrote a large part of the manuscript.

6.2 Approximated exponential integrators for the stochastic Manakov equation [12]

We present and study two exponential integrators for the stochastic Manakov equation (SME): the explicit exponential integrator (EE) and the symmetric exponential integrator (SE). We prove that the EE converges in the mean–square sense with order 1/2 in the case of a globally Lipschitz-continuous nonlinearity. Furthermore, we prove that the EE converges in probability with order 1/2 and almost surely with order 1/2− in the case of a cubic nonlinearity. We also present a nonhomogeneous version of the SME to illustrate the flexibility of the EE compared to the splitting schemes.

We present several numerical experiments comparing these novel exponential integrators to already existing numerical integrators. Numerically, we illustrate the order of convergence in the mean–square sense of the EE and SE integrators. Further, we illustrate the evolution of the solutions to the SME and a number of properties of the EE and SE. This includes how the SE preserves the $\mathbb{L}^2$-norm, the advantage in computational time of EE and SE, the strong order of convergence of EE in the inhomogeneous case, and the weak order of convergence of EE and SE.

Contributions: I reviewed and complemented a first draft of the work. I performed several numerical experiments, for instance the ones related to the Monte Carlo error estimates.

6.3 Lie–Trotter splitting for the nonlinear stochastic Manakov system [11]

We present and analyze the Lie–Trotter splitting integrator (LT) for the stochastic Manakov equation (SME). We prove that the LT converges in the mean–square sense with order 1/2 in the case of a globally Lipschitz-continuous nonlinearity. We also prove that the LT converges in probability with order 1/2 and almost surely with order 1/2− in the case of a cubic nonlinearity.

We perform several numerical experiments comparing the LT integrator to already existing numerical integrators. These numerical experiments include the orders of convergence in the mean–square, probability, and almost surely sense. We illustrate the evolution of solutions to the SME and their $\mathbb{H}^1$-norms. We also illustrate the Hamiltonian, mass center, and the pulse width of solitons. We also numerically illustrate the preservation property of

the LT and its advantage in computational time. Lastly, we generalize the SME nonlinearity and consider the critical exponents as with the SNLSE. We numerically investigate the critical exponent and conjecture that (in dimension 1) blowup occurs for $\sigma \geqslant 2$ in the deterministic case and for $\sigma > 2$ in the stochastic case.

Contributions: Together with my co-authors, I adapted the theoretical framework of [12] to prove convergence of the LT integrator. I wrote an extensive first draft. Furthermore, I designed, implemented and performed most of the numerical experiments.

6.4 Stochastic Generalized Benjamin–Bona–Mahony equations [10]

We apply the concept of exponential integrators to the stochastic generalized Benjamin–Bona–Mahony (SBBM) equation, introducing four exponential integrators in total: the explicit exponential integrator (EE), backward exponential integrator (BE), midpoint exponential integrator (ME), and symmetric exponential integrator (SE). We numerically compare these new integrators to several numerical schemes already introduced for the SBBM and BBM equations and investigate their properties. These numerical experiments consider both the BBM and SBBM, using a number of different coefficients. From the deterministic BBM equation to the stochastic SBBM equation, we illustrate the numerical schemes' respective convergence rates (in the deterministic, stochastic mean–square, probability, and almost surely senses) and preservation properties. Notable observations include that the SE and the Strang splitting integrator (ST) converge with order 2 in the deterministic and the linear stochastic case.

We also develop a method to numerically illustrate the order of convergence in probability in a concise manner.

Contributions: Aside from an initial selection of topics, and constructive criticism and critical eyes of my supervisors (main and co-), I have performed most work by myself.

Bibliography

[1] P. Agrawal G. *Nonlinear Fiber Optics*. Fourth. Elsevier/Academic Press, Amsterdam, 2006, p. 552. ISBN: 978-0-12-369516-1. DOI: 10.1016/B978-0-12-369516-1.X5000-6.

[2] P. Agrawal G. *Nonlinear Fiber Optics*. 5th ed. Academic Press, 2013. ISBN: 978-0-12-397023-7. DOI: 10.1016/C2011-0-00045-5.

[3] E. Allen. *Modeling with Itô Stochastic Differential Equations*. Vol. 22. Springer Science & Business Media, 2007. DOI: 10.1007/978-1-4020-5953-7.

[4] R. Anton. "Exponential Integrators for Stochastic Partial Differential Equations". PhD thesis. Umeå universitet, 2018. URL: http://urn.kb.se/resolve?urn=urn:nbn:se:umu:diva-146946.

[5] J. Avrin and J. A. Goldstein. "Global existence for the Benjamin-Bona-Mahony equation in arbitrary dimensions". In: *Nonlinear Analysis: Theory, Methods & Applications* 9.8 (1985), pp. 861–865. ISSN: 0362-546X. DOI: https://doi.org/10.1016/0362-546X(85)90023-9.

[6] L. Bachelier. *Louis Bachelier's Theory of Speculation: The Origins of Modern Finance*. Princeton University Press, Princeton Oxford, 2006. DOI: 10.1515/9781400829309.

[7] R. Belaouar, A. de Bouard, and A. Debussche. “Numerical analysis of the nonlinear Schrödinger equation with white noise dispersion”. In: *Stoch. Partial Differ. Equ. Anal. Comput.* 3.1 (2015), pp. 103–132. ISSN: 2194-0401. DOI: 10.1007/s40072-015-0044-z.

[8] T. B. Benjamin, J. L. Bona, and J. J. Mahony. “Model equations for long waves in nonlinear dispersive systems”. In: *Philosophical Transactions of the Royal Society of London. Series A, Mathematical and Physical Sciences* 272.1220 (1972), pp. 47–78. DOI: 10.1098/rsta.1972.0032.

[9] M. Benmiloud. *TikZBlog*. "https://latexdraw.com/draw-a-sphere-in-latex-using-tikz/". https://latexdraw.com/. May 2021.

[10] A. Berg. “Numerical simulations of stochastic generalized Benjamin–Bona–Mahony equations”. In: *N/A* (2023).

[11] A. Berg, D. Cohen, and G. Dujardin. “Lie–Trotter splitting for the nonlinear stochastic Manakov system”. In: *Journal of Scientific Computing* 88.1 (2021), pp. 1–31. DOI: 10.1007/s10915-021-01514-y.

[12] A. Berg, D. Cohen, and G. Dujardin. “Approximated exponential integrators for the stochastic Manakov equation”. In: *Journal of Computational Dynamics* (2023). ISSN: 2158-2491. DOI: 10.3934/jcd.2023002.

[13] A. Berg, D. Cohen, and G. Dujardin. “Numerical study of nonlinear Schrödinger equations with white noise dispersion”. In: *N/A* (2023).

[14] A. de Bouard and A. Debussche. “The nonlinear Schrödinger equation with white noise dispersion”. In: *J. Funct. Anal.* 259.5 (2010), pp. 1300–1321. ISSN: 0022-1236. DOI: 10.1016/j.jfa.2010.04.002.

[15] A. de Bouard and M. Gazeau. “A diffusion approximation theorem for a nonlinear PDE with application to random birefringent optical fibers”. In: *Ann. Appl. Probab.* 22.6 (2012), pp. 2460–2504. DOI: 10.1214/11-AAP839.

[16] R. W. Boyd. *Nonlinear Optics*. Third. Elsevier/Academic Press, Amsterdam, 2008, pp. xx+613. ISBN: 978-0-12-369470-6. URL: https://www.sciencedirect.com/book/9780123694706/nonlinear-optics.

[17] H. Brezis. *Functional Analysis, Sobolev Spaces and Partial Differential Equations*. Springer, 2011, pp. xiv+600. ISBN: 978-0-387-70914-7. DOI: 10.1007/978-0-387-70914-7.

[18] R. Camassa and D. D. Holm. "An integrable shallow water equation with peaked solitons". In: *Phys. Rev. Lett.* 71 (11 Sept. 1993), pp. 1661–1664. DOI: 10.1103/PhysRevLett.71.1661.

[19] R. A. Carmona and B. Rozovskii, eds. *Stochastic Partial Differential Equations: Six Perspectives*. Vol. 64. Mathematical Surveys and Monographs. American Mathematical Society, Providence, RI, 1999, pp. xii+334. ISBN: 0-8218-0806-0. DOI: 10.1090/surv/064.

[20] E. Celledoni, D. Cohen, and B. Owren. "Symmetric exponential integrators with an application to the cubic Schrödinger equation". In: *Foundations of Computational Mathematics* 8.3 (2008), pp. 303–317. DOI: 10.1007/s10208-007-9016-7.

[21] M. Chen, O. Goubet, and Y. Mammeri. "Generalized regularized long wave equation with white noise dispersion". In: *Stochastics and Partial Differential Equations: Analysis and Computations* 5.3 (2017), pp. 319–342. DOI: 10.1007/s40072-016-0089-7.

[22] D. Cohen and G. Dujardin. "Exponential integrators for nonlinear Schrödinger equations with white noise dispersion". In: *Stochastics and Partial Differential Equations: Analysis and Computations* 5.4 (2017), pp. 592–613. DOI: 10.1007/s40072-017-0098-1.

[23] D. Cohen and A. Lang. "Numerical approximation and simulation of the stochastic wave equation on the sphere". In: *Calcolo* 59.3 (Aug. 2022), p. 32. ISSN: 1126-5434. DOI: 10.1007/s10092-022-00472-7.

[24] E. D. Collett. "Polarized light. Fundamentals and applications". In: *Optical Engineering* (1993). URL: https://nla.gov.au/nla.cat-vn1133995.

[25] J. Cui et al. "Stochastic symplectic and multi-symplectic methods for nonlinear Schrödinger equation with white noise dispersion". In: *J. Comput. Phys.* 342 (2017), pp. 267–285. DOI: 10.1016/j.jcp.2017.04.029.

[26] G. Da Prato and J. Zabczyk. *Ergodicity for Infinite Dimensional Systems*. Vol. 229. Cambridge University Press, 1996. DOI: 10.1017/CBO9780511662829.

[27] G. Da Prato and J. Zabczyk. *Stochastic Equations in Infinite Dimensions*. 2nd ed. Encyclopedia of Mathematics and its Applications. Cambridge University Press, 2014. DOI: 10.1017/CBO9781107295513.

[28] F. Dalfovo et al. "Theory of Bose-Einstein condensation in trapped gases". In: *Rev. Mod. Phys.* 71 (3 Apr. 1999), pp. 463–512. DOI: 10.1103/RevModPhys.71.463.

[29] A. Debussche and Y. Tsutsumi. "1D quintic nonlinear Schrödinger equation with white noise dispersion". In: *J. Math. Pures Appl. (9)* 96.4 (2011), pp. 363–376. ISSN: 0021-7824. DOI: 10.1016/j.matpur.2011.02.002.

[30] B. Dörich and M. Hochbruck. "Exponential integrators for quasilinear wave-type equations". In: *SIAM Journal on Numerical Analysis* 60.3 (2022), pp. 1472–1493. DOI: 10.1137/21M1410579.

[31] Robert E., Thierry G., and Raphaèle H. "Finite volume methods". In: vol. 7. Handbook of Numerical Analysis. Elsevier, 2000, pp. 713–1018. DOI: https://doi.org/10.1016/S1570-8659(00)07005-8.

[32] M. Edwards and K. Burnett. "Numerical solution of the nonlinear Schrödinger equation for small samples of trapped neutral atoms". In: *Phys. Rev. A* 51 (2 Feb. 1995), pp. 1382–1386. DOI: 10.1103/PhysRevA.51.1382.

[33] K.-J. Engel, R. Nagel, and S. Brendle. *One-parameter Semigroups for Linear Evolution Equations*. Vol. 194. Springer, 2000, pp. xxi+589. ISBN: 978-0-387-98463-6. DOI: 10.1007/b97696.

[34] S.G. Evangelides et al. "Polarization multiplexing with solitons". In: *Journal of Lightwave Technology* 10.1 (1992), pp. 28–35. DOI: 10.1109/50.108732.

[35] G. Fenger, O. Goubet, and Y. Mammeri. "Numerical Analysis of the Midpoint Scheme for the Generalized Benjamin-Bona-Mahony Equation with White Noise Dispersion". In: *Communications in Computational Physics* 26.5 (2019), pp. 1397–1414. ISSN: 1991-7120. DOI: 10.4208/cicp.2019.js60.02.

[36] G. Fibich. *The Nonlinear Schrödinger Equation*. Vol. 192. Applied Mathematical Sciences. Singular solutions and optical collapse. Springer, Cham, 2015, pp. xxxii+862. ISBN: 978-3-319-12748-4. DOI: 10.1007/978-3-319-12748-4.

[37] C. Fu, C. N. Lu, and H. W. Yang. "Time–space fractional (2+ 1) (2 + 1) dimensional nonlinear Schrödinger equation for envelope gravity waves in baroclinic atmosphere and conservation laws as well as exact solutions". In: *Advances in Difference Equations* 2018.1 (2018), pp. 1–20. DOI: 10.1186/s13662-018-1512-3.

[38] L. Galati and S. Zheng. "Nonlinear Schrödinger equations for Bose-Einstein condensates". In: *AIP Conference Proceedings* 1562 (Oct. 2013), pp. 50–64. DOI: 10.1063/1.4828682.

[39] A. Galtarossa and C. Menyuk. *Polarization Mode Dispersion*. Jan. 2005. ISBN: 0-387-23193-5. DOI: 10.1007/b137385.

[40] C.S. Gardner and G. K. Morikawa. "Similarity in the asymptotic behavior of collision-free hydromagnetic waves and water waves". In: (May 1960). URL: https://www.osti.gov/biblio/4172979.

[41] J. Garnier and R. Marty. "Effective pulse dynamics in optical fibers with polarization mode dispersion". In: *Wave Motion* 43.7 (2006), pp. 544–560. ISSN: 0165-2125. DOI: 10.1016/j.wavemoti.2006.05.001.

[42] M. Gazeau. "Mathematical Analysis of Light Propagation in Optical Fibers with Randomly Varying Birefringence". PhD thesis. Ecole Polytechnique X, Oct. 2012. URL: https://pastel.archives-ouvertes.fr/pastel-00776990.

[43] M. Gazeau. "Probability and pathwise order of convergence of a semidiscrete scheme for the stochastic Manakov equation". In: *SIAM J. Numer. Anal.* 52.1 (2014), pp. 533–553. DOI: 10.1137/13090924X.

[44] B. Ghanbari, D. Baleanu, and M. Al Qurashi. "New Exact Solutions of the Generalized Benjamin-Bona-Mahony Equation". In: *Symmetry* 11.1 (2019). ISSN: 2073-8994. DOI: 10.3390/sym11010020.

[45] J. Ginibre and G. Velo. "The global Cauchy problem for the non linear Schrödinger equation revisited". In: *Annales de l'Institut Henri Poincaré C, Analyse non linéaire*. Vol. 2. 4. Elsevier. 1985, pp. 309–327. DOI: 10.1016/S0294-1449(16)30399-7.

[46] D. Gottlieb and S. A. Orszag. "Numerical Analysis of Spectral Methods". In: (1977). DOI: 10.1137/1.9781611970425.

[47] E. P. Gross. "Structure of a quantized vortex in boson systems". In: *Il Nuovo Cimento (1955-1965)* 20.3 (1961), pp. 454–477. DOI: 10.1007/BF02731494.

[48] J. Grue et al. "Formation of undular bores and solitary waves in the Strait of Malacca caused by the 26 December 2004 Indian Ocean tsunami". In: *Journal of Geophysical Research: Oceans* 113.C5 (2008). DOI: 10.1029/2007JC004343.

[49] N. Gücüyenen. "Strang splitting method to Benjamin–Bona–Mahony type equations: Analysis and application". In: *Journal of Computational and Applied Mathematics* 318 (2017). Computational and Mathematical Methods in Science and Engineering CMMSE-2015, pp. 616–623. ISSN: 0377-0427. DOI: 10.1016/j.cam.2015.11.015.

[50] Y. Guo, M. Wang, and Y. Tang. "Higher regularity of global attractor for a damped Benjamin–Bona–Mahony equation on R". In: *Applicable Analysis* 94.9 (2015), pp. 1766–1783. DOI: 10.1080/00036811.2014.946561.

[51] E. Hairer, C. Lubich, and G. Wanner. *Geometric Numerical Integration*. Second. Springer Series in Computational Mathematics. Structure-preserving algorithms for ordinary differential equations. Springer-Verlag, Berlin, 2006, pp. xvi+644. ISBN: 978-3-540-30663-4. DOI: 10.1007/3-540-30666-8.

[52] E. Hille and R. S. Phillips. *Functional Analysis and Semi-groups*. Vol. 31. American Mathematical Soc., 1996. ISBN: 978-0-8218-1031-6. DOI: 10.1090/coll/031.

[53] H. Holden et al. *Stochastic Partial Differential Equations*. Springer, 1996. ISBN: 978-0-387-89487-4. DOI: 10.1007/978-0-387-89488-1.

[54] J. Huang, Y. Tang, and M. Wang. "Singular support of the global attractor for a damped BBM equation". In: *Discrete and Continuous Dynamical Systems - B* 26.10 (2021), pp. 5321–5335. ISSN: 1531-3492. DOI: 10.3934/dcdsb.2020345.

[55] M. G. Hughes. "Application of a Non-Linear Shallow Water Theory to Swash following Bore Collapse on a Sandy Beach". In: *Journal of Coastal Research* 8.3 (1992), pp. 562–578. ISSN: 07490208, 15515036. URL: http://www.jstor.org/stable/4298006.

[56] R. S. Johnson. *A Modern Introduction to the Mathematical Theory of Water Waves*. 19. Cambridge university press, 1997. ISBN: 9780511624056. DOI: 10.1017/CBO9780511624056.

[57] T. Kato. "Nonlinear Schrödinger equations". In: *Schrödinger Operators*. Ed. by Helge Holden and Arne Jensen. Berlin, Heidelberg: Springer Berlin Heidelberg, 1989, pp. 218–263. ISBN: 978-3-540-46807-3. DOI: 10.1007/3-540-51783-9_22.

[58] S. Ken-Iti. *Lévy processes and infinitely divisible distributions*. Cambridge university press, 1999. ISBN: 9780521553025. URL: https://www.cambridge.org/se/academic/subjects/statistics-probability/probability-theory-and-stochastic-processes/levy-processes-and-infinitely-divisible-distributions.

[59] M. Kline. *Mathematical Thought from Ancient to Modern Times. Vol. 2*. Second. The Clarendon Press, Oxford University Press, New York, 1990, i–xx, 391–812 and i–xxii. ISBN: 0-19-506136-5. URL: https://search.ub.umu.se/permalink/46UMEA_INST/1v5n3j5/alma990001601930404996.

[60] P. E. Kloeden and E. Platen. *Numerical Solution of Stochastic Differential Equations*. Springer Berlin Heidelberg, 1992. DOI: 10.1007/978-3-662-12616-5.

[61] D. J. Korteweg and G. De Vries. "XLI. On the change of form of long waves advancing in a rectangular canal, and on a new type of long stationary waves". In: *The London, Edinburgh, and Dublin Philosophical Magazine and Journal of Science* 39.240 (1895), pp. 422–443. DOI: 10.1080/14786449508620739.

[62] M. Kovács and S. Larsson. "Introduction to stochastic partial differential equations". In: (2009). URL: https://research.chalmers.se/en/publication/79825.

[63] M. G. Larson and F. Bengzon. *The Finite Element Method: Theory, Implementation, and Applications*. Vol. 10. Springer Science & Business Media, 2013. ISBN: 978-3-642-33286-9. DOI: 10.1007/978-3-642-33287-6.

[64] B. Leimkuhler and S. Reich. *Simulating Hamiltonian Dynamics*. Vol. 14. Cambridge Monographs on Applied and Computational Mathematics. Cambridge University Press, Cambridge, 2005, pp. xvi+379. ISBN: 0-521-77290-7. DOI: 10.1017/CBO9780511614118.

[65] X. Leng and H. Chanson. "Effect of bed roughness on the propagation of negative surges in rivers and estuaries". In: *Proc., 21ème Congrès Français de Mécanique CFM 2013* (2013). URL: https://espace.library.uq.edu.au/view/UQ:307477.

[66] C. Lin et al. "Hydrodynamic features of an undular bore traveling on a 1: 20 sloping beach". In: *Water* 11.8 (2019), p. 1556. DOI: 10.3390/w11081556.

[67] G. Lindgren, H. Rootzén, and M. Sandsten. *Stationary Stochastic Processes for Scientists and Engineers*. English. Chapman and Hall, 2013. ISBN: 9781466586185. URL: https://portal.research.lu.se/en/publications/stationary-stochastic-processes-for-scientists-and-engineers.

[68] S. Manakov. "On the theory of two-dimensional stationary self-focusing of electromagnetic waves". In: *Soviet Physics-JETP* 38.2 (1974), pp. 248–253. URL: http://www.jetp.ras.ru/cgi-bin/e/index/e/38/2/p248?a=list.

[69] R. Marty. "Problèmes d'Évolution en Milieux Aléatoires: Théorèmes Limites, Schémas Numériques et Applications en Optique". PhD thesis. Toulouse 3, 2005. URL: https://api.semanticscholar.org/CorpusID:118200977.

[70] R. Marty. "On a splitting scheme for the nonlinear Schrödinger equation in a random medium". In: *Commun. Math. Sci.* 4.4 (2006), pp. 679–705. ISSN: 1539-6746. DOI: 10.4310/CMS.2006.v4.n4.a1.

[71] C. R. Menyuk. "Nonlinear pulse propagation in birefringent optical fibers". In: *IEEE Journal of Quantum Electronics* 23.2 (1987), pp. 174–176. DOI: 10.1109/JQE.1987.1073308.

[72] C. R. Menyuk. "Pulse Propagation in an Elliptically Birefringent Kerr Medium". In: *Quantum Electronics, IEEE Journal of* 25 (Jan. 1990), pp. 2674–2682. DOI: 10.1109/3.40656.

[73] C. R. Menyuk. "Application of multiple-length-scale methods to the study of optical fiber transmission". In: *J. Engrg. Math.* 36.1-2 (1999). Applications of solitons and symmetries, pp. 113–136. ISSN: 0022-0833. DOI: 10.1023/A:1017255407404.

[74] C. R. Menyuk and P. K. A. Wai. "Polarization evolution and dispersion in fibers with spatially varying birefringence". In: *JOSA B* 11 (July 1994), pp. 1288–1296. DOI: 10.1364/JOSAB.11.001288.

[75] C. R. Menyuk and P. K. A. Wai. "Polarization Mode Dispersion, Decorrelation, and Diffusion in Optical Fibers with Randomly Varying Birefringence". In: *Journal of Lightwave Technology* 14 (1996), pp. 148–157. DOI: 10.1109/50.482256.

[76] I. Neutelings. *University of Zürich CMS Wiki Pages*. "https://wiki.physik.uzh.ch/cms/latex:tikz:electromagnetic_wave". https://wiki.physik.uzh.ch/cms/latex:tikz:electromagnetic_wave. May 2018. URL: https://wiki.physik.uzh.ch/cms/latex:tikz:electromagnetic_wave.

[77] P. J. Olver. *Introduction to Partial Differential Equations*. Vol. 1. Springer, 2014, pp. xxv+636. ISBN: 978-3-319-02098-3. DOI: 10.1007/978-3-319-02099-0.

[78] M. Onorato et al. "Rogue Waves: From Nonlinear Schrödinger Breather Solutions to Sea-Keeping Test". In: *PLOS ONE* 8.2 (Feb. 2013), pp. 1–5. DOI: 10.1371/journal.pone.0054629.

[79] G. C. Papanicolaou and W. Kohler. "Asymptotic theory of mixing stochastic ordinary differential equations". In: *Communications on Pure and Applied Mathematics* 27.5 (1974), pp. 641–668. DOI: 10.1002/cpa.3160270503.

[80] A. Pazy. *Semigroups of Linear Operators and Applications to Partial Differential Equations*. Vol. 44. Springer New York, NY, 1983, pp. x+282. ISBN: 978-0-387-90845-8. DOI: 10.1007/978-1-4612-5561-1.

[81] D. H. Peregrine. "Calculations of the development of an undular bore". In: *Journal of Fluid Mechanics* 25.2 (1966), pp. 321–330. DOI: 10.1017/S0022112066001678.

[82] D. H. Peregrine. "Water waves, nonlinear Schrödinger equations and their solutions". In: *The Journal of the Australian Mathematical Society. Series B. Applied Mathematics* 25.1 (1983), pp. 16–43. DOI: 10.1017/S0334270000003891.

[83] L. P. Pitaevskii. "Vortex lines in an imperfect Bose gas". In: *Sov. Phys. JETP* 13.2 (1961), pp. 451–454. URL: http://www.jetp.ras.ru/cgi-bin/e/index/r/40/2/p646?a=list.

[84] H. Poincaré. "Théorie de la lumière". In: *Paris* 2 (1892). Ed. by M. Lamotte and D. Hurmuzescu. URL: https://archive.org/details/thoriemathma00poin/.

[85] H. Poincaré. "Traite de la lumiere". In: *Paris* 2 (1892), p. 165.

[86] C. Prévôt and M. Röckner. *A Concise Course on Stochastic Partial Differential Equations*. Vol. 1905. Springer, 2007. DOI: 10.1007/978-3-540-70781-3.

[87] G. N. Ramachandran and S. Ramaseshan. "Magneto-Optic Rotation in Birefringent Media—Application of the Poincaré Sphere". In: *J. Opt. Soc. Am.* 42.1 (Jan. 1952), pp. 49–56. DOI: 10.1364/JOSA.42.000049.

[88] M. Renardy and R. C. Rogers. *An introduction to Partial Differential Equations*. Vol. 13. Springer Science & Business Media, 2004, pp. xiv+434. ISBN: 978-0-387-00444-0. DOI: 10.1007/b97427.

[89] C. P. Robert, G. Casella, and G. Casella. *Monte Carlo Statistical Methods*. Vol. 2. Springer, 1999. ISBN: 978-0-387-21239-5. DOI: 10.1007/978-1-4757-4145-2.

[90] B. L. Rozovsky and S. V. Lototsky. "Stochastic evolution systems". In: *Probability Theory and Stochastic Modelling* 89 (1990). DOI: 10.1007/978-94-011-3830-7.

[91] B. L. Rozovsky and S. V. Lototsky. *Stochastic Evolution Systems: Linear Theory and Applications to Non-linear Filtering*. Vol. 89. Springer, 2018. DOI: 10.1007/978-3-319-94893-5.

[92] H. Shuqi and W. Kun. "Exponential integrator method for solving the nonlinear Helmholtz equation". In: *AIMS Mathematics* 7.9 (2022), pp. 17313–17326. ISSN: 2473-6988. DOI: 10.3934/math.2022953.

[93] N. F. Smyth and P. E. Holloway. "Hydraulic jump and undular bore formation on a shelf break". In: *Journal of Physical Oceanography* 18.7 (1988), pp. 947–962. DOI: 10.1175/1520-0485(1988)018<0947:HJAUBF>2.0.CO;2.

[94] M. Stanislavova. "On the global attractor for the damped Benjamin-Bona-Mahony equation". In: vol. 2005. Special. 2005, pp. 824–832. DOI: 10.3934/proc.2005.2005.824.

[95] G. Stewart. "On the wellposedness for periodic nonlinear Schrödinger equations with white noise dispersion". In: *Stochastics and Partial Differential Equations: Analysis and Computations* (2023), pp. 1–22. DOI: 10.1007/s40072-023-00306-9.

[96] W. A. Strauss. *Partial Differential Equations: An Introduction*. John Wiley & Sons, 2007. ISBN: 978-0-470-05456-7. URL: https://www.wiley.com/en-us/Partial+Differential+Equations%3A+An+Introduction%2C+2nd+Edition-p-9780470054567.

[97] C. Sulem and P. Sulem. *The Nonlinear Schrödinger Equation*. Vol. 139. Applied Mathematical Sciences. Self-focusing and wave collapse. Springer-Verlag, New York, 1999, pp. xvi+350. ISBN: 0-387-98611-1. DOI: 10.1007/b98958.

[98] Y. Tsutsumi. "L^2-solutions for nonlinear Schrödinger equations and nonlinear groups". In: *Funkcial. Ekvac.* 30.1 (1987), pp. 115–125. ISSN: 0532-8721. URL: http://www.math.sci.kobe-u.ac.jp/HOME/fe/xml/mr0915266.xml.

[99] M. Usman and B. Zhang. "Forced oscillations of a class of nonlinear dispersive wave equations and their stability". In: *Journal of Systems Science and Complexity* 20.2 (2007), pp. 284–292. DOI: 10.1007/s11424-007-9025-2.

[100] R. M. Vargas-Magaña, T. R. Marchant, and N. F. Smyth. "Numerical and analytical study of undular bores governed by the full water wave equations and bidirectional Whitham–Boussinesq equations". In: *Physics of Fluids* 33.6 (2021), p. 067105. DOI: 10.1063/5.0050067.

[101] J. B. Walsh. "An introduction to stochastic partial differential equations". In: *École d'Été de Probabilités de Saint Flour XIV - 1984*. Ed. by P. L. Hennequin. Berlin, Heidelberg: Springer Berlin Heidelberg, 1986, pp. 265–439. ISBN: 978-3-540-39781-6. DOI: 10.1007/BFb0074920.

[102] M. Wang. "Long time dynamics for a damped Benjamin–Bona–Mahony equation in low regularity spaces". In: *Nonlinear Analysis: Theory, Methods & Applications* 105 (2014), pp. 134–144. ISSN: 0362-546X. DOI: 10.1016/j.na.2014.04.013.

[103] M. Wang. "Long time behavior of a damped generalized BBM equation in low regularity spaces". In: *Mathematical Methods in the Applied Sciences* 38.18 (2015), pp. 4852–4866. DOI: 10.1002/mma.3400.

[104] H. Washimi and T. Taniuti. "Propagation of Ion-Acoustic Solitary Waves of Small Amplitude". In: *Phys. Rev. Lett.* 17 (19 Nov. 1966), pp. 996–998. DOI: 10.1103/PhysRevLett.17.996.

[105] G. B. Whitham. *Linear and Nonlinear Waves*. Pure and Applied Mathematics. Wiley-Interscience [John Wiley & Sons], New York-London-Sydney, 1974, pp. xvi+636. DOI: 10.1002/eqe.4290040514.